

The α -chemokine CXCL14 is up-regulated in the sciatic nerve of a mouse model of Charcot-Marie-Tooth disease type 1A and alters myelin gene expression in Schwann cells

Inaugural-Dissertation

zur

Erlangung des Doktorgrades der
Mathematisch-Naturwissenschaftlichen Fakultät
der Heinrich-Heine-Universität Düsseldorf

vorgelegt von

Elena Maria Barbaria

aus Mailand, Italien

Oktober 2008

Aus dem Institut für Molekulare Neurobiologie
der Heinrich-Heine-Universität Düsseldorf

Gedruckt mit der Genehmigung der Mathematisch-Naturwissenschaftlichen Fakultät
der Heinrich-Heine-Universität Düsseldorf

Referent: Prof. Dr. Hans Werner Müller

Koreferent: Prof. Dr. Heinz Mehlhorn

Tag der mündlichen Prüfung: 26. November 2008

“Considerate la vostra semenza:

fatti non foste a viver come bruti,

ma per seguir virtute e canoscenza“

Dante Alighieri, Divina Commedia, Inferno Canto XXVI

“People don't realise that molecules themselves are somewhat hypothetical, and that their interactions are more so, and that the biological reactions are even more so“

Kary Mullis, Nobel Prize in Chemistry 1993

Table of Contents

1. Abstract	9
1b. Zusammenfassung.....	11
2. Introduction.....	13
2.1 The myelin of the peripheral nervous system	13
2.2 The myelin proteins of the peripheral nervous system	13
2.3 PMP22.....	14
2.3.1 Cloning and expression of <i>PMP22</i>	14
2.3.2 Structure of PMP22.....	16
2.3.3 The <i>PMP22</i> gene.....	18
2.4 Regulation of PMP22.....	19
2.5 Other myelin proteins.....	21
2.5.1 P0 protein	21
2.5.2 Myelin basic protein.....	21
2.5.3 P2 protein	22
2.6 Charcot-Marie-Tooth disease.....	22
2.7 Classification of Charcot-Marie-Tooth neuropathies	23
2.8 Charcot-Marie-Tooth disease type 1	26
2.8.1 Charcot-Marie-Tooth disease type 1A	27
2.8.2 Charcot-Marie-Tooth disease type 1B	30
2.9 Other types of Charcot-Marie-Tooth disease type 1	31
2.9.1 Charcot-Marie-Tooth disease type 1C	31

2.9.2	Charcot-Marie-Tooth disease type 1D	31
2.9.3	Charcot-Marie-Tooth disease type 1F	32
2.10	Other hereditary neuropathies	32
2.10.1	Hereditary neuropathy with liability to pressure palsies	32
2.10.2	Dejerine-Sottas syndrome	33
2.10.3	Charcot-Marie-Tooth disease type X-linked dominant	34
2.10.4	Charcot-Marie-Tooth disease type 2	35
2.10.5	Charcot-Marie-Tooth disease type 4	35
2.11	Animal models of CMT	36
2.12	Animal models of CMT1A	37
2.12.1	Pmp22-transgenic rats	38
2.12.2	PMP22-transgenic mice	39
2.13	Recent advances using Charcot-Marie-Tooth disease animal models	40
2.13.1	Therapeutic approaches to Charcot-Marie-Tooth disease type 1A	40
2.13.2	Gene expression profiling	42
2.13.3	Inflammation as a contributing factor in Charcot-Marie-Tooth disease type 1	43
2.14	Aim of the thesis	44
3.	Material and Methods	46
3.1	Material	46
3.1.1	Reagents and kits	46
3.1.2	Antibodies	49
3.1.3	Devices and software	50
3.2	Methods	51

3.2.1 Animals	52
3.2.2 Genotype establishment	52
3.2.3 Tissue preservation for electron microscopy	54
3.2.4 Morphometry	54
3.2.5 Analysis of array data	55
3.2.6 Teased-nerve fibre preparation	55
3.2.7 Primary Schwann cell cultures.....	56
3.2.8 Immunofluorescence	57
3.2.9 Treatment with recombinant CXCL14 (rCXCL14).....	58
3.2.10 Cell proliferation assay	58
3.2.11 Plasmid preparation.....	59
3.2.12 Transfection of Schwann cells	61
3.2.13 RNA extraction	62
3.2.14 Quantitative RT-PCR (qRT-PCR)	64
3.2.15 Comparative Ct Method.....	66
4. Results.....	68
4.1 Myelin gene expression in the sciatic nerve	68
4.2 Morphometric analyses of peripheral nerves	70
4.3 Gene selection and expression study on selected genes	73
4.4 CXCL14 immunodetection in the sciatic nerve of PMP22tg mice.....	76
4.5 <i>Cxcl14</i> mRNA expression and CXCL14 immunolocalisation in cultured Schwann cells	80
4.6 Effect of rCXCL14 treatment on Schwann cells	82
4.7 Silencing of <i>Cxcl14</i> mRNA expression in Schwann cells	84

4.8 <i>Cxcl14</i> mRNA expression in other models of demyelinating inherited neuropathies.....	86
5. Discussion.....	88
6. References.....	93
7. Abbreviations.....	112
8. Acknowledgments.....	115

1. Abstract

Charcot-Marie-Tooth (CMT) disease is the most common human hereditary peripheral neuropathy, affecting approximately 1 in 2500 individuals. It is clinically characterised by progressive weakness and atrophy of the distal limb muscles. CMT type 1A (CMT1A), transmitted as an autosomal dominant trait, affects approximately 50% of all CMT patients. This disorder is mostly caused by a 1.5-Mb tandem duplication of chromosome 17, comprising the gene for the peripheral myelin protein 22-kDa (PMP22). Although there are numerous studies on the functional role of PMP22, the mechanisms of myelin degeneration under conditions of PMP22 overexpression are not entirely clear. Most of the transgenic animal models that were previously generated express multiple copies of PMP22 and are characterised by dysmyelination, a feature seen in patients with Dejerine-Sottas syndrome (DSS). As models for CMT1A, both a transgenic rat mutant and the mouse mutant C61 showed mild *PMP22* overexpression and slow progression of the disorder. Furthermore, histopathological features, such as de- and remyelination, hypermyelination and onion bulb formation, observed in the C61 mice, are similar to those seen in CMT1A patients. In order to investigate the mechanisms underlying *PMP22* overexpression-related demyelination in a model comparable to human CMT1A, the transgenic mouse line C61 was chosen for this study. These mice carry four copies of the human yeast artificial chromosome (YAC) clone 49G7 encompassing the entire human *PMP22* gene. In this thesis, analyses performed in the sciatic nerve of P7 C61 mice reveal up-regulation of myelin genes, as well as hypermyelination. Hypermyelinated fibres were previously described in CMT1A-patients, in the *Pmp22*-overexpressing rat as well as in adult PMP22-transgenic C61 mice, but they were never described before in a CMT1A model, at such young age. Hence, this study focuses on the early postnatal development of the peripheral nerves to

unveil any gene expression alteration that might have an impact on the early pathogenesis of CMT1A.

1b. Zusammenfassung

Das Charcot-Marie-Tooth (CMT) Syndrom ist bei einer durchschnittlichen Häufigkeit von 1:2500 die häufigste neurogenetische Krankheit. Die klinischen Symptome der CMT-Neuropathie sind progressive Schwäche und Muskelatrophie in den distalen Extremitäten. 50% der CMT-Patienten sind von CMT Typ 1A (CMT1A) betroffen. CMT1A ist eine Neuropathie mit autosomal dominantem Erbgang. Die meisten CMT1A-Patienten tragen eine 1,5 Mb Duplikation des Peripheral Myelin Protein 22-kDa (*PMP22*)-Gens. Trotz zahlreicher Studien der funktionellen Rolle des PMP22-Proteins sind die Mechanismen der *PMP22*-Überexpression verursachenden Myelindegeneration noch undeutlich. Bei den meisten transgenen Tiermodellen werden mehrere Kopien des *PMP22*-Gens exprimiert. Diese Modelle zeichnen sich durch Dysmyelinisierung aus, welches allerdings ein typisches Merkmal der Dejerine-Sottas-Syndrom Patienten ist. Es wurden auch zwei adäquate Tiermodelle für CMT1A generiert, die eine moderate *PMP22*-Überexpression und einen graduellen Ablauf der Krankheit zeigen. Beide transgenen Tiermodelle zeigen bei Demyelinisierung, Remyelinisierung, Hypermyelinisierung und Zwiebelschalenformationen einen ähnlichen Phänotyp wie bei der humanen CMT1A. Das Ziel dieser Arbeit ist die Analyse der Demyelinisierung in einem adäquaten CMT1A-Tiermodell, die durch eine *PMP22*-Überexpression verursacht wird. Die für die Studie ausgewählten transgenen Mäuse C61 tragen vier Kopien des Human Yeast Chromosome (YAC) Klones 49G7, der das komplette humane *PMP22*-Gen enthält. In dieser Arbeit wurden Analyse des Ischiasnervs von C61 Mäusen des Postnataltages 7 durchgeführt, die eine Überexpression der Myelinge und eine Hypermyelinisierung aufzeigen. Hypermyelinisierte Fasern wurden in zuvor durchgeführten Studien bei CMT1A-Patienten, in *Pmp22*-überexprimierenden Ratten, in adulten C61 Transgenen Mäusen aber nie in jungen CMT1A

Transgenen Tieren beschrieben. Daher visiert diese Arbeit die postnatale Frühentwicklung der Peripheren Nerven an, um Änderungen der Genexpression zu untersuchen, die sich früh auf die CMT1A-Pathogenese auswirken könnten.

2. Introduction

2.1 The myelin of the peripheral nervous system

Axons in vertebrates are uniquely surrounded by a myelin sheath. In the peripheral nervous system (PNS) the myelin sheath is produced by Schwann cells, which myelinate single axons. The myelin sheath is wrapped around the axons in segments (internodes) in which the glial membrane spirals around the axon with extrusion of the cytoplasmic contents and compaction, until adjacent cytoplasmic and external faces of the membrane directly appose each other. This peculiar structure gives myelin a high resistance and low capacitance. Large fibres may have as many as 50 concentric spirals of myelin and small fibres may have as few as 2 or 3. The compacted layered structure of myelin allows to reduce the current flows across the internodal membrane. Moreover, it focuses depolarisations, produced by action potentials, along the fibres on the periodic interruptions in the myelin (nodes of Ranvier), between adjacent internodes.

2.2 The myelin proteins of the peripheral nervous system

Most of the myelin internode consists of compact myelin. Abundant proteins include P0 protein, myelin basic protein (MBP), P2 protein and PMP22 in PNS myelin (Greenfield et al., 1973). Amino acid composition and biochemical properties identified P0 and PMP22 as integral membrane proteins, and MBP and P2 protein as extrinsic membrane proteins. P0 and PMP22 are positioned to maintain the periodicity of both the extracellular and cytoplasmic spacing of myelin membranes, while MBP and P2 could influence cytoplasmic leaflet fusion.

An unexpected finding of studies focussed on the elimination of myelin proteins in mice is that significant amounts of multilammellar membranes form in the absence of P0 (Giese et al., 1992), MBP (Privat et al., 1979), MAG (Li et al., 1994; Montag et al., 1994), PLP/MBP (Stoffel et al., 1997) or PLP/MBP/MAG (Uschkureit et al., 2000). Spiral expansion of myelin membranes, therefore, does not depend on these molecules. Electron microscopy, however, has convincingly established that P0 is essential for normal spacing of PNS compact myelin (Giese et al., 1992).

2.3 PMP22

PMP22 is a minor component of the myelin sheath of peripheral nerves. PMP22 belongs to a family of integral membrane glycoproteins that is characterised by four hydrophobic domains and conserved amino acid motifs (Jetten and Suter, 2000) which are evolutionary related. The proteins of this family are about 160 to 180 amino acid residues in size, and sequence comparisons suggest that the group may also include the claudins, components of tight junctions. PMP22 can be regarded as the prototypic member of the family. PMP22 plays a crucial functional role in peripheral nerves, based on the observation that genetic alterations in the PMP22 gene lead to various forms of myelination deficiencies in humans and rodents (Naef and Suter, 1998; Suter and Snipes, 1995).

2.3.1 Cloning and expression of PMP22

Cloning of *Pmp22* cDNA has been first described in the mouse as the result of a screening effort, aimed at the elucidation of the genetic program that regulates cellular growth arrest in fibroblasts. *Pmp22* was isolated as a transcript that was strongly up-regulated in quiescent NIH3T3 fibroblasts

and was called *gas-3* for growth-arrest specific mRNA number 3 (Ciccarelli et al., 1990; Manfioletti et al., 1990; Schneider et al., 1988). In 1991, the rat *Pmp22* cDNA was cloned, initially termed SR13 or CD25, based on two other differential screenings of cDNA libraries generated from injured versus non-injured sciatic nerves (De Leon et al., 1991; Spreyer et al., 1991; Welcher et al., 1991). It was then acknowledged that the corresponding bovine PMP22 protein had been described previously, together with P0, as one of two peripheral myelin specific glycoproteins, PASII and PASI, respectively, that stained with periodate-Schiff's reagent (Kitamura et al., 1976). Subsequently, the human *PMP22* cDNA was identified (Patel et al., 1992). In the last decade, the cloning of the cDNA of a *PMP22* orthologue in the zebrafish (Wulf et al., 1999) and a *PMP22*-related gene in *C. elegans* (Agostoni et al., 1999) have been reported. PMP22 is widely expressed in neural and non-neural tissues during embryonic development and in the adult (Baechner et al., 1995; De Leon et al., 1994; Kuhn et al., 1993; Lobsiger et al., 1996; Spreyer et al., 1991; Taylor et al., 1995; Welcher et al., 1991). In early embryonic PNS development of the rat, PMP22 is found in peripheral nerves and in dorsal root ganglia (DRG) from E12 onwards (Hagedorn et al., 1999). In contrast, expression in the early developing mouse DRG is very weak or absent (Paratore et al., 2002). Thus, PMP22 appears to be a valuable marker for PNS progenitors in rat embryos but not for early mouse neural crest derivatives. DRG sensory neurons and satellite cells continue to express PMP22 also into adulthood (De Leon et al., 1994). PMP22 is most highly expressed by myelinating Schwann cells and is strongly up-regulated in parallel with the initiation of myelination (Notterpek et al., 1999; Snipes et al., 1992). Immunohistochemical studies have localised PMP22 to the plasma membrane of non-myelinating and myelinating Schwann cells as well as to the compact portion of myelin (Haney et al., 1996; Snipes et al., 1992). Following sciatic nerve injury, PMP22 expression is rapidly down-regulated in the degenerating nerve segments distal to the site of injury but recovers

with nerve regeneration (De Leon et al., 1991; Kuhn et al., 1993; Snipes et al., 1992; Welcher et al., 1991). These data suggest that axons are required for high induction of PMP22 expression (Maier et al., 2002b). This hypothesis is supported by the finding that Schwann cells express low levels of PMP22 in the absence of neurons in culture. Only if myelin is formed, PMP22 expression increases strongly (Pareek et al., 1997). The majority of newly synthesised PMP22 in Schwann cells is rapidly degraded in the endoplasmic reticulum (Pareek et al., 1993). Only a minor portion of the synthesised PMP22 is glycosylated and accumulates in the Golgi apparatus. These proteins are translocated to the Schwann cell membrane in detectable amounts only when axonal contact and myelination occur. The rapid turnover of PMP22 in Schwann cells, however, is not altered by myelination. PMP22 is also found in the central nervous system (CNS) but at much lower levels than in peripheral nerves (De Leon et al., 1994; Parmantier et al., 1995). In the adult mouse, *Pmp22* mRNA levels are approximately 10-fold higher in sciatic nerve compared to the lung and intestine, and about 50 to 100-fold higher than in brain. Even lower levels are observed in testis, muscle and liver (Lobsiger et al., 1996; Spreyer et al., 1991; Suter and Patel, 1994; Taylor et al., 1995; Welcher et al., 1991). No PMP22 expression is found in preimplantation embryos (Fleming et al., 1997), but *Pmp22* expression is widespread in several ectodermal, endodermal, and mesodermal tissues during mouse development (Baechner et al., 1995).

2.3.2 Structure of PMP22

PMP22 encodes a hydrophobic integral membrane protein of 160 amino acids with a predicted molecular weight of approximately 18 kDa (Pareek et al., 1993; Patel et al., 1992; Sedzik et al., 1998; Spreyer et al., 1991; Suter et al., 1992b; Welcher et al., 1991). The protein consists of four

hydrophobic domains that fulfil the requirement for potential transmembrane domains. The PMP22 amino acid sequence is highly conserved between species, although not identical (Patel et al., 1992; Wulf et al., 1999). The putative intracellular domains of PMP22 are small and it appears unlikely that they are involved in specific interactions with intracellular proteins. The extracellular loops of PMP22 may directly interact with other molecules, but so far, no such extracellular interaction has conclusively shown, although direct association of PMP22 with P0 has been reported (D'Urso et al., 1999). Intracellularly, PMP22 associates in a glycosylation-dependent manner with the chaperon calnexin (Dickson et al., 2002). PMP22 has a single N-linked glycosylation chain attached to asparagine 41, as suggested by the appropriate consensus sequence in the primary PMP22 polypeptide. Human and cat PMP22 carry the HNK-1 carbohydrate epitope (Hammer et al., 1993; Snipes et al., 1993). This epitope has been identified previously as a sulfated glucuronic acid on other cell surface glycoproteins, including P0 (Schachner and Martini, 1995). Many of the proteins carrying the HNK-1 epitope function in cell-cell and cell-extracellular matrix adhesion, thus PMP22 might also be involved in adhesive processes, although strong homophilic protein-based PMP22-PMP22 interactions have been excluded (Takeda et al., 2001). PMP22 and P0 are similarly regulated during development and peripheral nerve injury and colocalise in compact myelin. The extracellular domain of P0 forms a tetramer with four molecules arranged around a central cavity (Shapiro et al., 1996) and PMP22 may be associated with this tetrameric complex (D'Urso et al., 1999; D'Urso and Muller, 1997). Such an association fits well with the fact that mutations affecting PMP22 or P0 are both associated with inherited demyelinating neuropathies (Berger et al., 2002; Muller, 2000), since the highly ordered structure and specific function of myelin implies a requirement for specific interactions between various myelin components (Scherer, 1997). Mutations or changes in the stoichiometry of these components are likely to affect the proper

structure and function of such protein complexes and offer also a hypothesis how changes in *PMP22* gene dosage may cause neuropathies (Snipes and Suter, 1995). Recently, it was revealed that PMP22 forms homodimers and also larger complexes (Tobler et al., 2002; Tobler et al., 1999), a process that might, in part, be stabilised by PMP22 glycosylation (Ryan et al., 2000). The exact functional implications of PMP22 oligomerisation remain unknown, but these processes are likely to play a role in disease processes in CMT1A, DSS or congenital hypomyelination (CH) caused by PMP22 point mutations (Tobler et al., 2002; Tobler et al., 1999).

2.3.3 The *PMP22* gene

The human *PMP22* gene spans approximately 40 kb and consists of six exons (Patel et al., 1992; Suter and Patel, 1994). Exons 1A and 1B are alternatively transcribed, resulting in two different mRNAs (Suter and Patel, 1994). Both transcripts encode the same PMP22 polypeptide but differ in the sequence of their 5' untranslated regions. Consequently, the expression of the two mRNAs is regulated by two different promoters P1 and P2. A possible additional promoter has been described, but its relevance in normal tissue remains to be determined (Huehne and Rautenstrauss, 2001). Exon 2 encodes the N-terminus, consisting of the first hydrophobic domain of PMP22. Exon 3 encodes the first extracellular loop, including the glycosylation site. Exon 4 encodes the second and half of the third hydrophobic domains. Exon 5 covers the remaining of the third domain, the second putative extracellular loop, the fourth hydrophobic domain, as well as the 3'-untranslated region. The human *PMP22* gene has been mapped to human chromosome 17p11.2-p12 (Patel et al., 1992), the mouse *Pmp22* gene to chromosome 11 (Suter et al., 1992a) and the rat *Pmp22* gene to 10q22 (Liehr and Rautenstrauss, 1995).

2.4 Regulation of PMP22

The expression of PMP22 is controlled by a combination of transcriptional and post-transcriptional mechanisms. Furthermore, there is an additional level of regulation affecting PMP22 protein stability and trafficking (Pareek et al., 1997), and the association of PMP22 with specific lipid rafts may be another regulatory aspect (Erne et al., 2002; Hasse et al., 2002). In particular, it has been suggested that certain myelin proteins might be transported in the same raft intracellularly, providing a platform for correct delivery to myelin. If PMP22 and P0 would be indeed associated in such common rafts, it may reinforce the concept of a strict requirement for correct stoichiometry of these two proteins. On the transcriptional level, two different promoters, P1 and P2, have been described; P1 appears to regulate myelinating Schwann cell-specific expression, while P2 is more ubiquitously active (Suter et al., 1994). Sequence characterisation of the promoter regions reveals that P1 contains a TATA-box-like element at the appropriate distance from the transcription initiation site. In contrast, no TATA-box-like sequence could be found in the P2 promoter. The immediate upstream sequence of the P2 promoter has a high GC content and resembles the promoter of a housekeeping gene. Progesterone activates specifically the *PMP22* promoter 1 in Schwann cell transfection assays (Desarnaud et al., 1998) and glucocorticosteroids stimulate both *PMP22* promoters in the same experimental paradigm (Desarnaud et al., 2000). The findings are consistent with studies demonstrating positive effects of sex steroid hormones on gene expression of *PMP22* (Melcangi et al., 2000). These results may also be related to the tantalising data that progesterone is beneficial for myelination in peripheral nerve regeneration (Koenig et al., 1995). Further transfection studies suggest that 300 bp upstream of the transcription initiation site on exon

1A contain the elements required for Schwann cell-specific expression (Saberan-Djoneidi et al., 2000). This minimal promoter activity appears to be under the control of a silencer element sensitive to cAMP (cyclic adenosine monophosphate), located between -0.3 kb and -3.5 kb from the start of transcription. Computer analysis of 2 kb of the promoter predicts several transcription factor binding sites, including CREB (cAMP responsive element binding protein; potentially involved in the response of *PMP22* expression to cAMP stimulation) and steroid receptors. The CREB binding element might be involved in silencing the *PMP22* promoter activity. A positive regulatory element is located just in front of promoter 1 and a prominent sequence-dependent DNA-protein complex was detected in electrophoretic mobility shift assays (Hai et al., 2001b). Site-directed mutagenesis of the binding region identified nucleotides at positions -46 to -43 as the crucial elements for the formation of the complex. Nucleotides at positions -46 and -45 were essential for transactivation. Such studies may provide the basis for competitive binding of triplex-forming oligonucleotides to regulate *PMP22* expression in vivo (Hai et al., 2001a), a potential gene therapy approach to normalise *PMP22* expression in CMT1A due to *PMP22* overexpression (Vallat et al., 1996). Although transfection studies in Schwann cells are informative, there are limitations since Schwann cells do not myelinate *in vitro*, unless they are co-cultured with neurons. Transgenic mice provide an ideal system to examine the cis-regulatory elements within the *PMP22* gene that are controlled by the intense axon-glia interactions in PNS development and during regeneration. 10 kb upstream of the *PMP22* translation start codon have been demonstrated to direct temporal and spatial expression in development and regeneration of peripheral nerves (Maier et al., 2002a). Post-transcriptional regulation of *PMP22* has also been suggested, but the responsible elements, which include the two different 5' and the 3'-untranslated regions, remain to be determined (Bosse et al., 1999).

2.5 Other myelin proteins

2.5.1 P0 protein

P0 constitutes 70% of the total proteins in PNS myelin. It is a type I transmembrane glycoprotein with a single extracellular immunoglobulin-like domain, one transmembrane domain, a cytoplasmic C-terminal, and an apparent molecular weight of 30 kDa (Lemke and Axel, 1985). When transfected into non-adherent cells in vitro, the extracellular domain of P0 protein mediated homophilic, but not heterophilic plasma membrane cell adhesion (D'Urso et al., 1990; Filbin et al., 1990). The extracellular domains of P0 interact as cis-linked tetramers that bind through hydrogen bonds to P0 tetramers in opposite orientation on the opposing plasma membrane. The intraperiod line of PNS myelin, therefore, is stabilised by P0 homophilic interaction in the same and opposing compact myelin membranes. Spacing between the extracellular leaflets of compact PNS myelin is altered in P0-null mice (Giese et al., 1992), but the major dense line is ultrastructurally similar to wildtype mice.

2.5.2 Myelin basic protein

MBP is localised at the cytoplasmic surface of both compact CNS and PNS myelin. It is a family of alternatively spliced, highly charged extrinsic membrane proteins (Greenfield et al., 1973; Zeller et al., 1984), which bind negatively charged lipids, especially phosphatidylserine residues. In MBP-

deficient shiverer mice, the cytoplasmic leaflets of compact CNS myelin are not fused (Privat et al., 1979). In contrast, the major dense line of PNS myelin is unaltered. MBP, therefore, maintains the major dense line of CNS but not of PNS myelin. It has been hypothesised that the positively charged cytoplasmic domain of P0 protein can maintain the major dense line of PNS myelin.

2.5.3 P2 protein

P2 is an extrinsic membrane protein that is enriched in compact PNS myelin. P2 has also been detected in CNS myelin of rabbits and humans (Trapp et al., 1983), but not in mice or rats. The reasons for the species differences are unknown. P2 protein can induce an autoimmune PNS demyelinating disease when injected subcutaneously with complete Freund's adjuvant (Kadlubowski et al., 1980). P2 protein has never been eliminated from the mouse genome and P2 spontaneous mutations in rodent or humans have never been identified. P2 belongs to a family of proteins that function in fatty acid transport (Uyemura et al., 1984). It may also participate in fusion of the major dense line of compact PNS myelin.

2.6 Charcot-Marie-Tooth disease

Hereditary peripheral neuropathies affect approximately 1 in 2500 people and are among the most common inherited diseases of the nervous system. Based on clinical, neurophysiological and neuropathological features, hereditary neuropathies have been classified into hereditary motor and sensory neuropathies (HMSNs), hereditary sensory and autonomic neuropathies (HSANs) and hereditary motor neuropathies (HMNs). HMSNs are also known as Charcot-Marie-Tooth disease

and related neuropathies, named after the authors who, in 1886 independently described a syndrome characterised by a slowly progressive, distal sensorimotor process beginning in childhood. Clinically, CMT neuropathies are characterised by onset in childhood or early adulthood, distal weakness, sensory loss, foot deformities (pes cavus and hammertoes) and absent reflexes. On the basis of neurophysiological properties and neuropathology, CMT has been divided into primary demyelinating and axonal types. Most CMT neuropathies are demyelinating, although up to one third appear to be primary axonal disorders. The primary demyelinating neuropathies include CMT1 as well as Dejerine-Sottas syndrome, congenital hypomyelination and hereditary neuropathy with liability to pressure palsies (HNPP). The primary axonal neuropathies have been classified as CMT2. Most CMT neuropathies of both the demyelinating and the axonal type show autosomal dominant inheritance, although X-linked dominant (CMTX) and autosomal recessive forms (CMT4) have been also described. Apparent sporadic cases exist, because dominantly inherited disorders may begin as a consequence of a new mutation. At least 35 genes are known to cause inherited neuropathies, and more than 50 distinct loci have been identified. The inherited peripheral neuropathies mutation database (www.molgen.ua.ac.be/CMTMutations/default.cfm) provides a comprehensive and updated list of all known mutations.

2.7 Classification of Charcot-Marie-Tooth neuropathies

HMSNs are now best known and classified as CMT and related neuropathies. The CMT neuropathies may be subdivided into a group with motor nerve conduction velocity (NCV) below 38 m/s (CMT1) and a group with motor NCV above 38 m/s (CMT2). In general, this classification based on electrophysiological findings is still valid, although molecular genetics studies allowed

further definition of demyelinating CMT. In fact, CMT and related neuropathies can be divided into CMT1 if the patient has an autosomal dominant demyelinating neuropathy, CMT2 if the neuropathy is dominantly inherited and axonal, CMTX if the patient has an X-linked neuropathy and CMT4 if the neuropathy is recessive. As some families show NCVs that make it difficult to assign the label CMT1 or CMT2 and display typical autosomal dominant inheritance, the term dominant intermediate Charcot-Marie-Tooth disease (DI-CMT) was also recently introduced. The importance of Schwann cell-axonal interactions and the molecular architecture of both myelin and the axons are crucial in the pathogenesis of CMT (Suter and Scherer, 2003). Figure 1 is particularly significant to represent this concept.

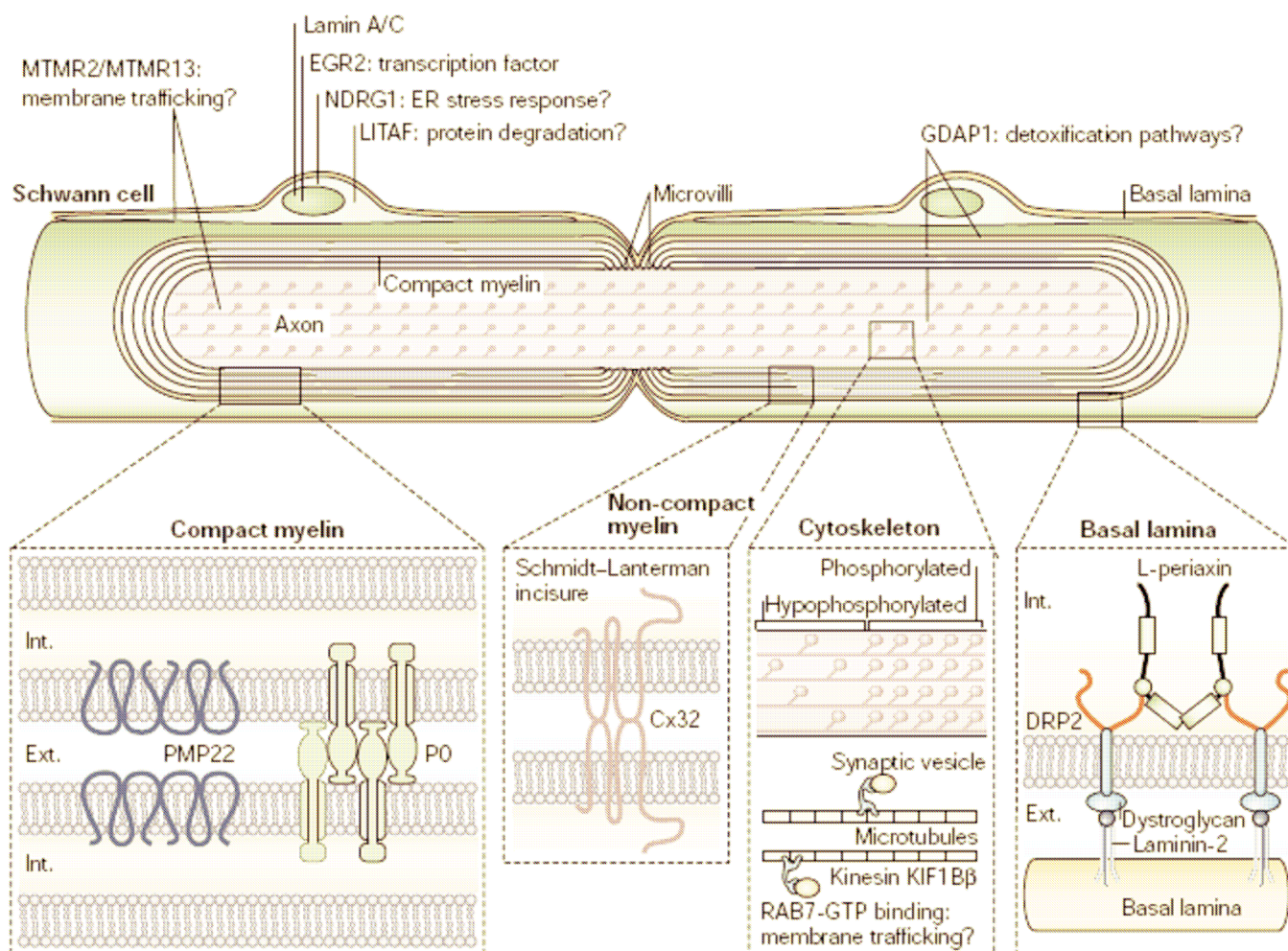


Figure 1. The figure shows the locations of the wildtype proteins encoded by the genes that are mutated in CMT. Cx, connexin; EGR, early growth response; ER, endoplasmic reticulum; Ext., extracellular; GDAP, ganglioside induced differentiation-associated protein; Int., intracellular; KIF, kinesin family member; LITAF, lipopolysaccharide-induced tumour necrosis factor (TNF)- α factor; MTMR, myotubularin-related protein; NDRG, N-myc downstream-regulated gene; PMP, peripheral myelin protein (Suter and Scherer, 2003).

2.8 Charcot-Marie-Tooth disease type 1

CMT1 patients show slowly progressive distal muscle weakness and wasting, initially affecting the small foot and peroneal muscles. Later in the disease course, weakness and wasting of the small hand muscles may appear. Sensory loss is variable and affects both large and small fibre modalities. Deep tendon reflexes are almost invariably absent in CMT1 patients. Most patients show foot deformities, like high arches and hammertoes (Fig. 2)

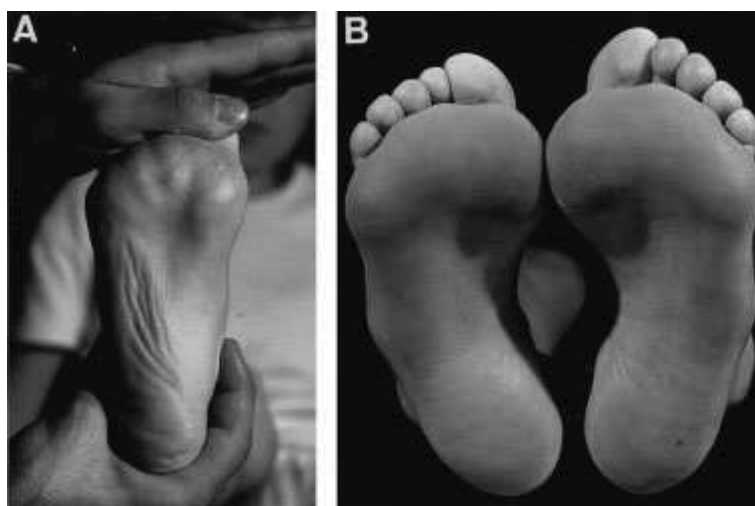


Figure 2. (A) Sole of the foot shows incipient pes cavus, abductor hallucis (AH) muscle atrophy, and flattening of transverse arcus plantaris in a 6-year-old affected boy. (B) For comparative purposes, the feet in this 13-year-old affected boy shows advanced pes cavus and varus, complete flattening of transverse arcus plantaris, and atrophy of the AH muscles; callosity is present along the external border of the foot (Berciano et al., 2003).

The course of CMT1 is usually benign and most patients remain ambulatory throughout life. Additional features, including postural tremor (Roussy-Levy syndrome) and muscle cramps may occur. Occasional patients develop a severe phenotype in infancy and others develop minimal disability during their life. The presence of mutations in genes other than *PMP22* may account for this clinical variability. Slowing of NCV below 38 m/s is part of the definition of CMT1. However, a variable degree of axonal damage is also present in CMT1 and is responsible for the severity of clinical impairment. Often, sensory action potentials are so severely reduced that they are not even recordable. Chronic denervation is usually observed by electromyography (EMG). In 1991 the first genetic mutation causing a distinct form of CMT1 was described (Lupski et al., 1991). Since then, several other mutations in genes expressed by myelinating Schwann cells have been found.

2.8.1 Charcot-Marie-Tooth disease type 1A

CMT1A is the most typical form of CMT1. It is caused by a 1.5 megabase tandem duplication on chromosome 17p11.2, containing the gene encoding *PMP22* (Lupski et al., 1991). Approximately 60% of CMT1 patients have this duplication. Almost all *de novo* CMT1A duplications are caused by an unequal crossing-over event during spermatogenesis. Both sides of the CMT1A duplication are flanked by highly homologous proximal and distal tandem repeat sequences. Misalignment of the CMT1A repeat sequences during meiosis causes the CMT1A duplication. One of the two resulting haploid spermatocytes contains two copies of the *PMP22* gene (duplication) and the other one does not contain any copy of it (deletion). The deletion of the *PMP22* gene may then explain the genotype of HNPP. Several pieces of evidence confirm the role of the *PMP22* gene and of its duplication in causing CMT1A: 1) naturally occurring mouse models of CMT1A (Trembler and

TremblerJ) are caused by missense mutations in the *PMP22* gene; 2) transgenic mice and rats bearing extra copies of the *PMP22* gene develop a CMT1A-like neuropathy; 3) some patients with missense mutations in the *PMP22* gene develop a similar phenotype; 4) patients homozygous for the duplication are usually more severely affected than heterozygous ones. PMP22 is overexpressed in CMT1A nerve biopsies, suggesting that an increased level of PMP22 is the most likely pathogenic mechanism for CMT1A. The mechanisms by which an increased PMP22 dose leads to CMT1A are still unclear. Overexpression of PMP22 may affect Schwann cell maturation and differentiation, leading to altered myelin formation and subsequent demyelination. A role for immune-mediated demyelination has been also proposed in an animal model of CMT1A, as for connexin 32 (*Cx32*) and myelin protein zero (*MPZ*) mutations (Kobsar et al., 2005). Neurophysiological and neuropathological studies suggest that axonal damage plays a relevant role in CMT1A neuropathy (Hanemann and Gabreels-Festen, 2002). The pathomechanisms of axonal impairment in CMT1A are unknown. Morphological studies in sural nerves from patients with duplications of the *PMP22* gene show reduced density of myelinated fibres and most of the remaining myelinated fibres are surrounded by 'onion bulbs', made up of concentric layers of Schwann cell cytoplasm, that wrap around thinly or almost normally myelinated axons (Fig. 3).

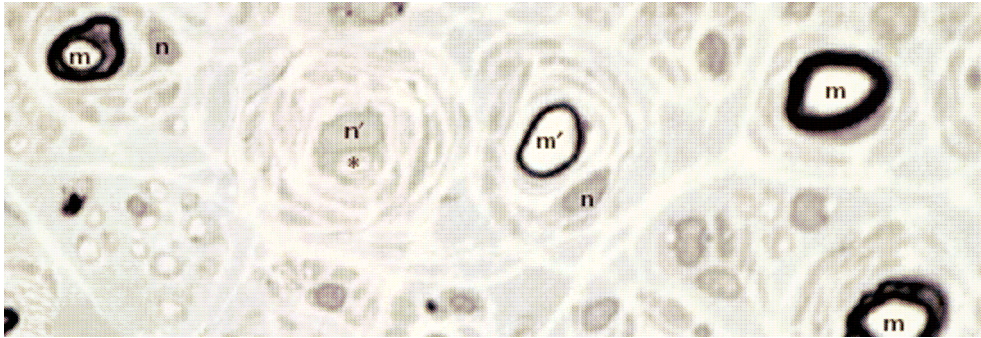


Figure 3. Microphotograph of a semi-thin section of a sural nerve biopsy from a 46-year-old patient with CMT1A. Note the supernumerary Schwann cell processes and their nuclei (n) that form 'onion bulbs' around demyelinated and remyelinated axons, and the reduced density of myelinated axons (m). m', thinly myelinated axons; asterisk indicates demyelinated axons and n' indicates their associated Schwann cell nuclei (Suter and Scherer, 2003).

As expected in a demyelinating disease, unmyelinated fibre density appears normal or only mildly reduced. Morphometric studies show that larger fibres are more affected than smaller ones. The mean internodal length is reduced, demonstrating that remyelination is prominent in nerve fibres of CMT1A patients.

Neuropathies caused by *PMP22* missense mutations are relatively rare and often severer than those caused by duplication of the gene. The pathology of these cases is also severer, though direct genotype-phenotype correlations are not possible.

Inflammatory changes may be observed in sural nerve biopsies of CMT1A patients. This observation suggest a concomitant inflammatory process. There is some evidence in animal models to support a macrophage-mediated process underlying demyelination in the early stages of CMT1A (Kobsar et al., 2005).

2.8.2 Charcot-Marie-Tooth disease type 1B

CMT1B occurs less often than CMT1A, accounting for 4-5% of all CMT1 cases, and is caused by various mutations in the gene encoding P0 on chromosome 1. Patients with CMT1B show a variety of phenotypes. Many neuropathies caused by *MPZ* gene mutations tend to cluster with early onset or late onset neuropathies (Shy et al., 2004). The mechanism by which different mutations in the *MPZ* gene cause distinct phenotypes is unclear. The type and location of the mutation on the *MPZ* coding region may determine the severity of the neuropathy. In typical CMT1B cases, the sural nerve biopsy shows a variable loss of myelinated fibres, onion bulbs and segmental demyelination in teased fibres. Focal thickenings of the myelin sheath have been observed in CMT1B patients. In other families, ultrastructural examination shows uncompacted myelin in several fibres, thus

suggesting two divergent neuropathological phenotypes in CMT1B, the first dominated by myelin thickenings and the second by loosening of myelin lamellae. Morphometric studies show a preferential loss of larger fibres, like in CMT1A. Most remaining fibres, outside of the myelin thickenings have high g-ratios, thus confirming the severity of the demyelinating process (Gabreels-Festen et al., 1996). Axonal degeneration is the prominent feature of nerve biopsies from patients with late onset disease and demyelination is less evident. Most biopsies show marked loss of myelinated fibres of all calibres, with numerous clusters of regenerating axons.

2.9 Other types of Charcot-Marie-Tooth disease type 1

2.9.1 Charcot-Marie-Tooth disease type 1C

CMT1C is caused by mutations in the lipopolysaccharide-induced tumour necrosis factor (*LITAF*) gene, also known as small integral membrane protein of lysosome/late endosome (*SIMPLE*). The function of the *LITAF/SIMPLE* gene is unknown, as are the mechanisms underlying CMT1C. These patients develop distal muscle weakness and atrophy, sensory loss and slow nerve conduction velocities. The neuropathological abnormalities are suggestive of a hypertrophic demyelinating neuropathy, like CMT1A. In particular, myelin loss and onion bulbs similar to those observed in CMT1A have been reported in one large family with CMT1C (Street et al., 2003)

2.9.2 Charcot-Marie-Tooth disease type 1D

Mutations in the early growth response 2 (*EGR2*, also called *KROX20*) gene, a transcription factor involved in the regulation of myelination cause CMT1D. Variable phenotypes are associated with *EGR2* gene mutations. Most patients are severely affected, but milder cases with an adult onset have been described (Shy, 2004). Patients with CMT1D display neuropathological changes ranging from severe to relatively mild loss of myelinated fibres. Onion bulbs are present but they are not as prominent as in CMT1A. Fibres showing a reduced axon diameter compared with myelin thickness have also been observed, consistent with axonal atrophy.

2.9.3 Charcot-Marie-Tooth disease type 1F

A particular type of autosomal dominant demyelinating neuropathy may be also caused by mutations in the neurofilament light chain (*NEFL*) gene. These patients are normally severely affected and may show signs of axonal damage. Families exclusively showing axonal features have been classified as having CMT2E.

2.10 Other hereditary neuropathies

2.10.1 Hereditary neuropathy with liability to pressure palsies

HNPP is an autosomal dominant demyelinating neuropathy caused by a deletion of the 17p11.2 chromosomal region, which is duplicated in CMT1A (Chance et al., 1993). HNPP is characterised by recurrent episodes of peripheral nerve palsies caused by mechanical compression or trauma of

the nerve trunks. Electrophysiological studies have shown nerve conduction slowing, prolonged distal latencies and sometimes conduction blocks. The examination of sural nerve biopsies discloses a variable number of sausage-like thickenings of the myelin sheath (tomacula) with a near-normal number of myelinated fibres. At the electron microscopic level, tomacula look like redundant loops of myelin with irregularly folded lamellae, which are also enormously increased in number. Rarely, HNPP sural nerves show a severe reduction of myelinated fibres and a high number of onion bulbs. These unusual patients have been reported to develop a clinical and neurophysiological phenotype indistinguishable from CMT1. Some cases of HNPP may be also caused by point mutations of the *PMP22* gene, often leading to insertion of a stop codon or a frameshift (Shy, 2004). Because only one copy of the *PMP22* gene is present in HNPP patients and *PMP22* underexpression at both the messenger RNA and the protein levels have been demonstrated, a gene dosage mechanism has been proposed as the most likely pathogenic factor for the disease. How down-regulation of *PMP22* leads to HNPP is, however, still unknown.

2.10.2 Dejerine-Sottas syndrome

Dejerine-Sottas syndrome is probably not a distinct clinical and genetic entity. However, the term is useful to describe a hypertrophic demyelinating polyneuropathy with early onset and a severe disabling clinical course, whose genotype may be caused by point mutations in different genes (*PMP22*, *MPZ*, *EGR2* and periaxin). DSS is normally caused by autosomal dominant or dominant *de novo* mutations. Rarely, a homozygous mutation either in the *PMP22* or in the *MPZ* gene has been described. Motor NCV is markedly lowered and sensory NCV is usually not recordable. Nerve biopsy shows a profound loss of myelinated fibres and a diffuse formation of onion bulbs.

Occasionally, onion bulbs around demyelinated axons are made up only of concentric layers of basal lamina.

2.10.3 Charcot-Marie-Tooth disease type X-linked dominant

In CMTX the inheritance pattern has classic X-linked features, like the absence of male-to-male transmission. CMTX is the second most common form of CMT, accounting for 10-16% of cases. A severer clinical course and a significant lowering of motor NCV in males compared with females characterise CMTX. CMT1X is the most common type of CMTX and is caused by missense mutations in the *CX32KD* gene, encoding connexin 32 (also known as gap junction- β 1), located on the X chromosome. Connexin 32 is a major component of non-compact myelin at the nodes of Ranvier and Schmidt-Lanterman incisures. This protein presumably plays a role in the gap junction formation, permitting the passage of small molecules and ions between adjacent loops of the paranode or incisures. This neuropathy is caused by primary axonal damage with possible secondary demyelination and the severity of the neuropathy is related to the degree of axonal loss (Shy, 2004). The neuropathology of CMTX differs from that of CMT1A and CMT1B, as it is mainly characterised by axonal changes, with atrophy and clusters of axonal regeneration and minimal signs of de/remyelination. Electron microscopy analysis reveals widening of the Schmidt-Lanterman incisures and of the nodes of Ranvier, along with a separation of the myelin sheath from the axon that leaves a clear periaxonal space appearing either empty or filled with vesicular material whose significance is unknown (Hahn et al., 2001).

2.10.4 Charcot-Marie-Tooth disease type 2

The phenotype of CMT2 is similar to that of CMT1, with distal weakness and atrophy, distal sensory loss and foot deformities. Therefore, a distinction between the two forms based only on clinical features is impossible. However, CMT2 patients have a wider range of symptom onset and degree of disability than those with CMT1. CMT2 is the axonal form and displays NCVs above 38 m/s. CMT2 is dominantly inherited and includes approximately 30% of autosomal dominant CMT. The discovery of the guanosine triphosphatase mitofusin 2 gene (*MFN2*) mutations in most CMT2 patients (CMT2A) is important because there is finally a mutated gene to test in CMT2 families (Reilly, 2005). The neuropathological phenotype of most CMT2 patients is similar. In sural nerve biopsies, the number of myelinated fibres is only mildly decreased, particularly for large diameter fibres. Occasionally, clusters of small regenerating fibres or small onion bulbs may be seen. Irregular foldings of the myelin sheath have been rarely described. Teased fibres preparations have often shown fibres with short internodes, but there has been no evidence of clear segmental demyelination.

2.10.5 Charcot-Marie-Tooth disease type 4

The autosomal recessive forms of CMT1 have been classically defined as CMT4. However, axonal types were recently included in the CMT4 type, therefore this term should be referred to as autosomal recessive CMT irrespective of the demyelinating or axonal nature. CMT4 are rare and have heterogenous phenotypes. Usually CMT4 neuropathies are severer than the autosomal

dominantly inherited ones. They may have systemic symptoms, such as cataracts and deafness. Multiple subtypes of CMT4 may be identified based on molecular genetic tests.

2.11 Animal models of CMT

Animals models covering the most frequent forms of human CMT are now available (Table 1).

CMT models with altered expression of Pmp22 and Mpz have been most intensively studied.

Human mutation	Clinical presentation	Related genetic models (mouse unless stated)	Animal mutation	Model for	Reference
PMP22 duplication	CMT1	PMP22 tg rat (CMT rat) PMP22 tg (C61, C22) PMP22 tg (TgN248) PMP22 tg My41)	mouse PMP22 cosmid tg human PMP22 YAC tg mouse PMP22 cosmid tg mouse PMP22 YAC tg	CMT1A CMT1A/CH DSN DSN	[6] [15,16] [17] [18]
PMP22 point mutation	CMT1, DSN, CH	Trembler Trembler-J Trembler-Ncnp Trembler-m1H Trembler-m2H PMP22 KO	spont PMP22 point mut G150D spont PMP22 point mut L16P spont PMP22 ex IV del mutagen PMP22 point mut H12R mutagen PMP22 point mut Y153X	DSN DSN DSN DSN DSN	[7] [19] [20] [21] [21]
PMP22 deletion	HNPP	PMP22 KO	PMP22 ex II replaced by NeoR	HNPP	[22,23]
MPZ point mutation	CMT1, CMT2, DSN	MPZ het null MPZ null MPZ tg (80.2, 80.4) MPZ I106L tg MPZ S63C tg MPZ S63del tg MPZ S63del tg in MPZ het null	MPZ NeoR-ins MPZ neo-ins mouse MPZ tg MPZ I106L tg MPZ S63C tg MPZ S63del tg MPZ S63del tg in MPZ het null	mild CMT1B DSN CH severe CMT1B CMT1B CMT1B CMT1B	[5] [24] [25] [26] [27*] [27*] [27*]
Cx32/GJB1 point mut	CMTX, CMT2	Cx32 null Cx32 frameshift mutant	Cx32 ex 2 NeoR ins Cx32(R142W) tg	CMTX CMTX	[28] [29]
EGR2 point mutation	CMT1, DSN, CH	EGR2 null EGR2lo/lo	EGR2 LacZ-Neo ins EGR2 floxed neoR in intron1	CH CH	[30] [31]
PRX point mutation	CMT4F, DSN	PRX null	PRX ex 6-7 NeoR ins	CMT4F	[32]
MTMR2 point mutation	CMT4B	MTMR2 null MTMR2 null	MTMR2 ex 4 floxed/CMV-Cre MTMR2 stop E276X, ex 9-13 repl LacZ-tkNEO	CMT4B1 CMT4B1	[33] [34*]
KIF1B point mut	CMT2A (1 family)	KIF1B het null	KIF1B neoR ins	CMT2A	[35]
NEFL point mut	CMT2E	NEFL L394P tg	NEFL L394P tg	severe CMT2E	[36]
LMNA	AR-CMT2	LMNA null	LMNA neoR ins	AR-CMT2	[37]

Table 1. Models representing the most common forms of human inherited neuropathies.

PMP22, peripheral myelin protein 22kDa; CMT, Charcot-Marie-Tooth disease; tg, transgene; YAC, yeast artificial chromosome; CH, congenital hypomyelination; DSN, Dejerine-Sottas neuropathy (also called DSS); mut, mutation; ex, exon; HNPP, hereditary neuropathy with liability to pressure palsies; MPZ, myelin protein zero; ins, insert; het, heterozygous; Cx32, connexin 32; GJB1, gap junction β 1; EGR2, early growth response gene 2; PRX, periaxin; MTMR2, myotubularin related protein 2; repl, replaced; KIF1B, kinesin family member 1B; NEFL, neurofilament light chain; LMNA, lamin A/C (Meyer Zu Hörste and Nave, 2006).

2.12 Animal models of CMT1A

The spontaneous mouse mutants Trembler and TremblerJ both carry point mutations in the *Pmp22* gene (Suter et al., 1992a; Suter et al., 1992b) and share pathological features with CMT1A. The same mutation has been identified in mouse and in one human CMT1A family (Valentijn et al., 1992). However, the subcellular consequences of *Pmp22* misfolding in trembler mice and *PMP22* overexpression in the majority of CMT1A cases are different (Giambonini-Brugnoli et al., 2005), therefore trembler mice cannot be considered as models for human CMT1A. Overexpression of wildtype *Pmp22* can only be modelled by transgenic extra copies of the wildtype gene. Transgenic animals are generated by injection of purified DNA restriction fragments or larger genomic fragments, such as yeast artificial chromosomes (YACs) or bacterial artificial chromosomes (BACs) into fertilised oocytes. Recombination of the cloned DNA into the host genome is random. Typically, the integration process creates multiple copies of smaller transgene fragments that are then found in a tandem head-to-tail orientation. For smaller transgenes there is also a poor correlation between copy number and gene expression level, as expression level may depend on positional effects. Both *Pmp22*-overexpressing rats and mice have been generated (Huxley et al., 1996; Huxley et al., 1998; Magyar et al., 1996; Robertson et al., 2002; Sereda et al., 1996; Sereda et al., 2003). The CMT-like phenotype of these rodents was the first direct proof that in humans *PMP22* is the responsible gene within the duplicated 1.5 Mb region. Rodents with moderately increased *Pmp22* mRNA provide models for the human disease CMT1A, whereas higher expression levels lead to severe manifestation of peripheral neuropathy, similar to Dejerine-Sottas syndrome or even congenital hypomyelination. Mice in which *Pmp22* overexpression was first turned on and then off could demonstrate that the *Pmp22*-overexpression dependent demyelination

is reversible (Perea et al., 2001), a finding of principle interest for research aimed at reducing *PMP22* overexpression pharmacologically.

2.12.1 *Pmp22*-transgenic rats

The *Pmp22*-overexpressing rat was generated by pronuclear injection of a cosmid-derived 43 kb DNA fragment, containing the entire murine *Pmp22* gene (Sereda et al., 1996). The same construct was used also for the generation of a transgenic mouse model (Magyar et al., 1996). In the transgenic rat, approximately three additional copies of the genomic fragment were autosomally transmitted. However, the degree of transcriptional *Pmp22* overexpression was only 1.6-fold (Sereda et al., 2003). All *Pmp22* transgenic rats showed signs of dysmyelination and demyelination in peripheral and cranial nerves (Grandis et al., 2004; Sereda et al., 1996). Onion bulbs could also be detected at the age of 2.5 months. In agreement with the clinical phenotype, motor fibres were more severely affected than sensory fibres. Moreover, large calibre axons were more severely hypomyelinated than small calibre fibres (Sereda et al., 1996). A clinical phenotype was obvious at about 3 weeks of age. Electrophysiologically, adult CMT rats exhibited a slowing of motor nerve conduction velocity, with values similar to those of CMT1A patients. Axonal loss and distally pronounced muscle atrophy matched the human CMT1A symptoms (Sereda et al., 2003). Minor differences of transcriptional *Pmp22* overexpression can have significant impact on the development and course of disease. When *Pmp22* transgenic rats were bred to homozygosity, *Pmp22* mRNA expression increased accordingly, causing a dramatic increase of clinical severity. (Niemann et al., 2000). Homozygous animals died prematurely, most probably as a result of respiratory insufficiency, as the peripheral nervous system was virtually amyelinated. At the ultra-

structural level, Schwann cells were able to single-out individual axons, but appeared arrested at the promyelin stage. The failure to assemble myelin contrasted with an ongoing differentiation at the molecular level, which included the transcription of myelin genes (Niemann et al., 2000).

2.12.2 *PMP22-transgenic mice*

A 43 kb cosmid-derived DNA fragment harbouring the murine *Pmp22* gene was used for the generation of transgenic mice. Lines with either 16 or 30 transgene copies were obtained (Magyar et al., 1996). These mice exhibited a very similar and severe dysmyelinated phenotype. At the mRNA level, *Pmp22* was two-fold up-regulated, but only when normalised to *Mpz* mRNA, as both messages were reduced in sciatic nerve RNA. This is in contrast to the elevated expression of *Pmp22* mRNA in the *Pmp22*-overexpressing rat. Myelin was absent from the majority of axons in histological sections, yet most Schwann cells were associated 1 : 1 with axons at the promyelin stage. This degree of dysmyelination is very similar to that of homozygous *Pmp22*-overexpressing rats (Niemann et al., 2000). Schwann cells remained immature, with reduced overall myelin gene expression and elevated proliferation. Classical onion bulbs were not a feature. These mice confirm the gene dosage hypothesis for CMT1A, but represent a model for the more severe Dejerine-Sottas syndrome.

Huxley and colleagues generated several lines of *PMP22* transgenic mice by pronuclear injection of a YAC, containing the 40 kb human *PMP22* gene (Huxley et al., 1996; Huxley et al., 1998). One line (C22), with about eight YAC copies, had a strong behavioural phenotype at 3 weeks of age, followed by progressive hind-limb weakness. Histologically, there was pronounced absence of myelin and occasional basal laminal onion bulbs, both of which were thought to result from

demyelination and remyelination. *PMP22* overexpression was estimated to be 2.7-fold at the RNA level. The C61 line results from the same series of YAC-transgenic mice and harbours four copies of the human *PMP22* gene. The C61 mice exhibit a lower degree of *PMP22* overexpression and show no major signs of motor impairment. When analysed in more detail, younger C61 mice (age 2 months) revealed reduced muscle strength and deficits in motor coordination and balancing (Norreel et al., 2001). Histologically, the development of peripheral myelin was initially normal, but followed by demyelination, mainly of larger calibre axons, at approximately 4 weeks of age (Robertson et al., 1999; Robertson et al., 2002). Electron microscopy of sciatic nerves taken from 14-week-old mice revealed demyelinated and thinly remyelinated axons, supernumerary Schwann cells as well as hypermyelinated small calibre axons, a pattern very similar to the morphological description of the *Pmp22*-overexpressing rats. Electrophysiologically, NCV were reduced (Huxley et al., 1998) and F-wave latencies measured in the sciatic nerve were prolonged compared with wildtype controls, confirming another clinical feature of CMT1A (Kobsar et al., 2005). Kobsar and colleagues also reported a peculiar involvement of invading B and T cells, which were observed previously in other mice with demyelinating neuropathies. Taken together, these data indicate that the C61 line represents an useful mouse model for human CMT1A.

2.13 Recent advances using Charcot-Marie-Tooth disease animal models

2.13.1 Therapeutic approaches to Charcot-Marie-Tooth disease type 1A

Recently, three different treatment strategies for CMT1A were preclinically tested and found to be promising in animal models. The first approach took advantage of the knowledge that the *PMP22*

gene in Schwann cells is under partial control of progesterone (Koenig et al., 1995; Schumacher et al., 2001). Administration of progesterone activates the *PMP22* gene *in vitro* (Desarnaud et al., 1998) and increases *PMP22* and *MPZ* expression *in vivo* (Melcangi et al., 1999; Sereda et al., 2003). In contrast, subcutaneous application of the selective progesterone receptor antagonist onapristone reduced total *Pmp22* expression in peripheral nerves of *Pmp22*-overexpressing rats (Sereda et al., 2003). This reduction was small at the mRNA level, but sufficient to reduce axon loss and to improve adult muscle strength, also after prolonged treatment (Meyer Zu Hörste and Nave, 2006). However, continued intake of progesterone-containing drugs appears problematic in CMT1A patients.

The second approach uses ascorbic acid and appears remarkably simple. Ascorbic acid (vitamin C) is an antioxidant that is also required for extracellular matrix formation and myelination by Schwann cells, at least *in vitro* (Podratz et al., 2001; Podratz et al., 2004). In the C22 transgenic mouse line, the weekly oral application of ascorbic acid reduced the percentage of severely hypomyelinated axons. Moreover, ascorbic acid improved the motor performance in different tests and even reduced premature death of C22 mice (Passage et al., 2004). Clinical trials with ascorbic acid are now under way in CMT1A patients (Pareyson et al., 2006).

Since axon loss is a common feature of neuropathies, therapeutic strategies involve neurotrophins. Neurotrophin-3 is synthesised in normal Schwann cells, promotes nerve regeneration after injury and, in synergy with insulin-like growth factor-2 and platelet-derived growth factor, the survival of Schwann cells in the absence of axons (Meier et al., 1999). Using nude mice with an implanted CMT1A nerve xenograft (as well as dysmyelinated TremblerJ mice), the application of neurotrophin-3 had a positive effect (Sahenk et al., 2005). Subcutaneous application of neurotrophin-3 three times a week improved axonal regeneration and remyelination of axons,

mostly in small calibre fibres (<2 μm). Concurrently, a clinical pilot study was performed with recombinant neurotrophin-3 in a small group of CMT1A patients. Six months of treatment increased the density of Schwann cells and myelinated axons in sural nerve biopsies of CMT1A patients. Moreover, treated patients exhibited improved sensory functions and a reduced neurological impairment score (Sahenk et al., 2005). This is the first report of a successful treatment of CMT1A in humans, and illustrates how clinical research benefits from animal models.

2.13.2 Gene expression profiling

Gene expression profiles have been obtained from nerve samples of CMT1A animal models and have given insights into underlying genetic perturbations of development. In one study (Vigo et al., 2005), a cDNA microarray analysis of 30-day-old homozygous *Pmp22*-overexpressing rats, compared with wildtype rats, demonstrated a transcriptional down-regulation of genes involved in cell cycle regulation, lipid and glucose metabolism, extracellular matrix formation and myelination. In contrast, transcripts related to cell proliferation were up-regulated.

In another study, using a serial analysis of gene expression (SAGE)-cDNA library from adult *PMP22* transgenic C22 mice, ten Asbroek and colleagues reported reduced expression of genes for myelination, protein synthesis, extracellular matrix, and the cytoskeleton (ten Asbroek et al., 2005). Both studies by Vigo et al. and by ten Asbroek et al. reported the down-regulation of mRNA for ciliary neurotrophic factor (*CNTF*). This neurotrophin is synthesised by Schwann cells (Sendtner et al., 1990) and is known to be downregulated in inflammatory neuropathies (Ito et al., 2001). Lack of Schwann cell-derived CNTF may contribute to axon loss and CMT pathology.

A further microarray analysis compared gene expression profiles in nerves from young (P4) and adult (P60) Trembler, C22 *PMP22*-transgenic mice and homozygous *Pmp22*-null mice (Giambonini-Brugnoli et al., 2005). C22 and Trembler revealed a massive reduction of cholesterol biosynthesis, reflecting a reduced synthesis rate of cholesterol-rich myelin membranes. Trembler mice had up-regulated expression of heat shock and other stress response proteins. In *Pmp22*-null mice, transcripts with known functions in cell cycle regulation and DNA replication were increased. In C22 mice, reduced myelin gene expression appeared uncoupled from Schwann cell differentiation, as previously described at the protein level in homozygous *Pmp22*-overexpressing rats (Niemann et al., 2000). It is difficult in these studies, however, to distinguish primary molecular defects from many secondary alterations of gene expression and from the final common pathway of all CMT diseases.

2.13.3 Inflammation as a contributing factor in Charcot-Marie-Tooth disease type 1

A series of experimental studies have provided evidence that T lymphocytes and macrophages are a pathologically relevant feature of demyelination when caused by mutation in myelin genes, at least in CMT1 mouse models. An increased number of CD8-positive T lymphocytes and macrophages was found in peripheral nerves of *P0*, *PMP22* and gap junction protein *Cx32* mutant mice (Berghoff et al., 2005; Kobsar et al., 2005; Schmid et al., 2000). The macrophages were found to be mainly resident endoneural macrophages (Kobsar et al., 2003). Myelin mutant mice were cross-bred with mice deficient in the recombination activating gene 1 (*RAG-1*) (Kobsar et al., 2003; Mäurer et al., 2003; Schmid et al., 2000) and the T-cell receptor α -subunit (*TCR α*) (Mäurer et al., 2003). By genetically abolishing functional T lymphocytes, pathological demyelination was reduced and nerve

conduction velocities were improved in heterozygous P0^{-/-} mice (Schmid et al., 2000). Peripheral demyelination in this P0 model was equally reduced by deleting the macrophage adhesion protein sialoadhesin (Kobsar et al., 2006) and the macrophage colony stimulating factor (*M-CSF*) (Carenini et al., 2001). Interestingly, also in Cx32 mutant mice, myelin pathology and axonal size reduction were ameliorated by concurrent RAG-1 deficiency (Kobsar et al., 2003). Early onset dysmyelination modelled by homozygous P0 deficiency was, unlike demyelination, not ameliorated by lack of T lymphocytes (Berghoff et al., 2005). These findings indicate that immune reactions may aggravate genetically determined demyelination, independently of the underlying mutation. It was hypothesised that an unstable pathological myelin sheath could constitute an immunogenic target leading to its progressive destruction by activated macrophages. Schwann cells may secrete chemokines attracting macrophages and lymphocytes (Kobsar et al., 2005). Successful treatment of CMT animal models by pharmacological modulation of the immune system, however, has been so far not reported. Possible benefits of an antiinflammatory treatment in CMT patients remain controversial (Martini and Toyka, 2004).

2.14 Aim of the thesis

Despite the several aforementioned studies, the pathogenesis of CMT1A neuropathy, caused by the over-expression of *PMP22*, has not yet been entirely understood. Therefore, the aim of this thesis was to investigate the molecular mechanisms underlying demyelination, by using the C61 mouse model, which is a suitable animal model that mimics the human CMT1A disorder.

First, myelin gene expression was analysed in the sciatic nerve of C61 and wildtype mice, and the results were compared with the morphology of the peripheral nerves. Then, in order to identify

genes other than *PMP22* that might have a role in the pathogenesis of CMT1A, few putatively interesting genes were chosen from a list of candidates for further analyses. Among these genes, the gene encoding the α -chemokine CXCL14 was most prominently up-regulated in the sciatic nerve of C61 mice. Hence, the localisation of CXCL14 both *in vivo* and *in vitro* were examined to confirm the expression of this chemokine by Schwann cells. Furthermore, by using cultured Schwann cells, the function of CXCL14 was investigated. The purpose of these latter experiments was not only to understand the role of CXCL14 in normal conditions, but also to clarify the significance and the possible consequences of the transcript up-regulation observed in the CMT1A animal model. Ultimately, the findings here reported aim to demonstrate the functional relevance of CXCL14 in Schwann cell myelination and possibly in the pathogenesis of CMT1A.

3. Material and Methods

3.1 Material

3.1.1 Reagents and kits

Name	Company
Ampicillin	Sigma-Aldrich, Munich, Germany
Collagenase type I	Sigma-Aldrich, Munich, Germany
Ethidium bromide solution 1% (1 mg/ml)	Roth, Karlsruhe, Germany
Deoxyribonuclease I, Amplification Grade	Invitrogen, Karlsruhe, Germany
Dulbecco's Modified Eagle's Medium (DMEM)	Invitrogen, Karlsruhe, Germany
EndoFree Plasmid Maxi Kit	Qiagen, Hilden, Germany
Foetal calf serum	PAA Laboratories, Pasching, Germany

Fluoromont-G	SouthernBiotech (Biozol Diagnostica), Eching, Germany
Forskolin	Sigma-Aldrich, Munich, Germany
FuGENE HD Transfection Reagent	Roche Applied Science, Mannheim, Germany
HotStarTaq Master Mix	Qiagen, Hilden, Germany
Hygromycin	Sigma-Aldrich, Munich, Germany
L-Glutamine	Invitrogen, Karlsruhe, Germany
LiChrosolv Water	Merck, Darmstadt, Germany
Normal goat serum	Sigma-Aldrich, Munich, Germany
One Shot® TOP10 Chemically Competent E. coli	Invitrogen, Karlsruhe, Germany
Penicillin/Streptomycin (Penicillin G sodium/Streptomycin Sulfate)	Invitrogen, Karlsruhe, Germany
Pentobarbital	Essex Pharma, Munich, Germany

Phosphate buffered saline (PBS)	Invitrogen, Karlsruhe, Germany
Poly-D-lysine	Sigma-Aldrich, Munich, Germany
Power SYBR® Green PCR Master Mix	Applied Biosystems, Darmstadt, Germany
Primers	Eurofins MWG Operon, Ebersberg, Germany
Proteinase K PCR Grade	Roche Applied Science, Mannheim, Germany
Random primers	Invitrogen, Karlsruhe, Germany
Recombinant Mouse Cxcl14/BRAK	R&D Systems, Wiesbaden, Germany
RNeasy Mini Kit	Qiagen, Hilden, Germany
Superscript II Reverse Transcriptase	Invitrogen, Karlsruhe, Germany
TRIZOL Reagent	Invitrogen, Karlsruhe, Germany
Trypsin/EDTA (1x) 0.05%	Invitrogen, Karlsruhe, Germany

<i>Cxcl14</i> -specific shRNAs and control vectors	OriGene, Rockville, MD, USA
<i>p57kip2</i> -suppression vector (H1- <i>kip2</i>) and control vector	Gift of Dr. Patrick Küry
pcDNA3-hyg-citrine vector	Gift of Dr. Patrick Küry
4',6-diamidino-2-phenylindole (DAPI)	Roche Applied Science, Mannheim, Germany
5-Bromo-2'-deoxy-uridine Labeling and Detection Kit I	Roche Applied Science, Mannheim, Germany

3.1.2 Antibodies

Name	Host	Company
Anti-CXCL14/BRAK pAb	Sheep	R&D Systems, Wiesbaden, Germany
Anti-CXCL14/BRAK mAb (Clone 135633)	Rat	R&D Systems, Wiesbaden, Germany
Anti-neurofilament (Pan-cocktail)	Rabbit	Biotrend, Cologne, Germany

Anti-S100	Rabbit	Abcam, Cambridge, UK
Anti-F4/80 biotin-conjugated	Rat	Serotec, Eching, Germany
Anti-CD34 biotin-conjugated	Rat	BD Pharmingen, San Jose, CA, USA
Anti-sheep Alexa Fluor® 488	Donkey	Invitrogen, Karlsruhe, Germany
Anti-rat Alexa Fluor® 488	Goat	Invitrogen, Karlsruhe, Germany
Anti-rabbit Alexa Fluor® 594	Goat	Invitrogen, Karlsruhe, Germany
Streptavidin Cy3		Cedarlane, Burlington, Ontario, Canada

3.1.3 Devices and software

Ultrathin sections were investigated using a ProScan Slow Scan CCD camera mounted to a Leo 906 E electron microscope (Zeiss, Oberkochen, Germany) and the corresponding software iTEM (Soft Imaging System, Münster, Germany).

Immunofluorescence images were acquired on an Axioplan 2 microscope using the AxioVision 4.2 software (Zeiss, Oberkochen, Germany).

For proliferation assays, Schwann cell counting was performed on an Eclipse TE 200 microscope, using the Lucia 4.21 software (Nikon, Düsseldorf, Germany).

Centrifugation steps for Schwann cell preparation were carried out in an Eppendorf 5804 centrifuge (Eppendorf, Hamburg, Germany).

Centrifugation steps for RNA extraction were carried out in an Eppendorf 5417R centrifuge (Eppendorf, Hamburg, Germany).

Centrifugation steps for plasmid preparation were carried out in a Sorvall RC5B Plus centrifuge (Thermo Scientific, Oberhausen, Germany).

Peripheral nerves were homogenised using a Polytron PT-MR2100 homogeniser (Kinematica, Lucerne, Switzerland).

DNA and RNA concentrations were determined by using a Nanodrop ND-1000UV/Vis spectrophotometer (Peqlab, Erlangen, Germany).

PCR reactions for mouse genotyping were carried out in a Biometra TRIO Thermoblock (Biometra, Göttingen, Germany).

Agarose gels were visualised by using a camera mounted on a UV transilluminator and images were acquired using the corresponding software Diana v1.6 (Ray Test, Straubenhardt, Germany).

qRT-PCR reactions were carried out with a 7000 Real-Time PCR System (Applied Biosystems, Darmstadt, Germany). Data were acquired using SDS 2.0 software (Applied Biosystems, Darmstadt, Germany).

3.2 Methods

3.2.1 Animals

Transgenic PMP22-overexpressing mice of the C61 strain (PMP22tg) carrying four copies of a human YAC clone encompassing the complete human *PMP22* gene (Huxley et al., 1996; Huxley et al., 1998) were obtained from the Mammalian Genetics Unit, Medical Research Council, Harwell (UK). Heterozygous C61 mice were bred in the animal facility of Heinrich-Heine-Universität Düsseldorf, by crossing a heterozygous male with a wildtype female. Animals were kept under pathogen-free conditions, at constant temperature of 21°C and humidity of 50% ± 5, on a 12h light/dark cycle. All animal handling and experimental procedures described in this thesis were conducted in compliance with the German Animal Protection Law.

3.2.2 Genotype establishment

In order to confirm the genotype of newborn mice, a small fragment of the tail was digested in lysis buffer (50 mM KCl, 10 mM Tris-HCl pH 8.3, 2.5mM MgCl₂, 0.45% Tween 20, 0.45% Triton X-100. Sterilised by filtration), supplemented with 1 mg/ml proteinase K, at 60°C overnight. Digested tails were incubated at 99°C for 10 minutes for DNA denaturation and then 1.5 µl of digested tissue, containing genomic DNA, was used as a template in a PCR (polymerase chain reaction).

Primers specific for human *PMP22* gene were used to identify transgenic heterozygous mice. As internal control, primers specific for mouse β-actin were used in the same PCR.

Primers are listed below.

	Forward Primer	Reverse Primer
Human <i>PMP22</i>	TCAGGATATCTATCTGATTCTC	AAGCTCATGGAGCACAAAACC
Mouse β -actin	AACCGTGAAAAGATGACCC	TCGTTGCCAATAGTGATGACC

The PCR reaction mixture was prepared as described in the table below.

	Initial Concentration	Final Concentration	Volume (μ l)
Human <i>PMP22</i> forward primer	25 μ M	0.5 μ M	1
Human <i>PMP22</i> reverse primer	25 μ M	0.5 μ M	1
Mouse β -actin forward primer	25 μ M	0.5 μ M	1
Mouse β -actin reverse primer	25 μ M	0.5 μ M	1
HotStarTaq Master Mix	2x	1x	25
LiChrosolv water to 50 μ l			19
Template (gDNA)			1.5
Total Volume			50

PCR protocol: 95°C for 15 min, *95°C for 30 s, 55°C for 30 s, 72°C for 1 min*, from* to* repeat for 38 cycles; 72°C for 10 min, 4°C. PCR reactions were carried out in a Biometra TRIO Thermoblock.

At the end of the PCR, 10 μ l of 6x Orange G-based loading buffer (30% glycerol, 2 mg/ml Orange G) was added to each sample and 22 μ l of each of them were loaded onto a 2% agarose gel

containing 5 % (v/v) ethidium bromide. Gel was visualised by using a camera mounted on a UV transilluminator and images were acquired using the software Diana v1.6.

3.2.3 Tissue preservation for electron microscopy

PMP22tg mice and their wildtype littermates were decapitated at postnatal day 7. The skin was cut ventral and dorsal at the inguinal region and the whole animals were fixed in 2% paraformaldehyde and 2% glutaraldehyde in 0.1 M cacodylate buffer overnight at 4°C. Mouse tails were kept and frozen for genotyping. The next day, femoral nerves composed of the motor quadriceps and cutaneous saphenous branch, as well as sciatic nerves were taken, osmified and embedded in Spurr's medium. For electron microscopy, ultrathin sections of 70 nm thickness were counterstained with lead citrate and investigated using a Zeiss Leo 906 E electron microscope.

3.2.4 Morphometry

Ultrathin sections of peripheral nerves of PMP22tg mice and their wildtype littermates (n=5) were investigated with regard to myelin, sorting of axons (ratio axon : Schwann cell = 1:1), axonal calibre and g-ratio, using a ProScan Slow Scan CCD camera mounted to a Zeiss Leo 906 E electron microscope and the corresponding software iTEM. For g-ratio, 100 completely myelinated axons per mouse, in 1:1 ratio with Schwann cells were examined.

3.2.5 Analysis of array data

Affymetrix Gene Chip Mouse Expression Arrays 430A (Affymetrix, Santa Clara, CA, USA) were formerly used in our laboratory to compare sciatic nerve cDNA expression of wildtype and PMP22tg mice at postnatal day 7.

Data were subsequently analysed by using the software ArrayAssist 4.0 (Stratagene, Amsterdam, Netherlands) with five different algorithms: MAS5.0 (Affymetrix, Santa Clara, CA, USA), MBEI (Li and Wong, 2001), PLIER (Affymetrix, Santa Clara, CA, USA), RMA (Irizarry et al., 2003) and GCRMA (Wu, 2004). After variance stabilisation (+16) and log-transformation (base 2) statistical analysis was carried out via t-test. The thresholds to consider genes to be regulated were > 1.1 (fold-change) and < 0.05 (p-values). Genes were considered significantly regulated if they satisfied the given criteria by three algorithms, including either PLIER or GCRMA.

3.2.6 Teased-nerve fibre preparation

One-month-old transgenic mice and their wildtype littermates were anaesthetised with sodium pentobarbital (50 mg/kg). Under deep anaesthesia, mice were transcardially perfused with 10 ml of 1x phosphate-buffered saline (1x PBS: NaCl 136.9 mM, KCl 2.7 mM, KH_2PO_4 1.5 mM, Na_2HPO_4 7.7 mM; pH 7.4), followed by 10 ml of 2% paraformaldehyde in PBS. The skin was cut dorsally, sciatic nerves were exposed and dissected, washed in PBS and incubated in 0.5-fold PBS. Nerves were manually unsheathed from epineurium and teased into single fibres, using a pair of fine forceps on frost-resistant slides. Slides were dried overnight at room temperature and then stored at -20°C , for subsequent staining.

3.2.7 Primary Schwann cell cultures

Rat Schwann cells were prepared from sciatic nerves of neonatal Wistar rats and purified by complement lysis as described previously (Brockes et al., 1979). Briefly, neonatal rats (1–2 days old) were killed by decapitation, pinned out in a laminar flow hood with dorsal side uppermost and washed with 70% ethanol. The sciatic nerves were dissected free up to the sciatic notch, cut out and stored in 0.02 M HEPES at pH 7.2 at room temperature. The nerves were transferred to a sterile beaker and incubated for 15 min at 37 °C in 3 ml of medium containing 0.25% trypsin and 0.03% collagenase in 0.02 M HEPES at pH 7.2. At the end of this period, the supernatant was decanted and the procedure repeated twice. After the final digestion, 2 ml of supernatant was removed and 1 ml of 10% (v/v) foetal calf serum was added. The nerves were dissociated by 3 cycles of trituration through a number-23 hypodermic needle. The turbid suspension was passed through a sterile square of nylon gauze to remove debris, and centrifuged at 500 g for 10 min at room temperature. The supernatant was removed and the pellet resuspended in 10% foetal calf serum. The cells were plated into tissue culture flasks coated with 100 µg/ml poly-D-lysine and incubated at 37°C and 10% CO₂. Cultures were expanded in DMEM (Dulbecco's modified Eagle's medium) supplemented with 10% (v/v) foetal calf serum, 50 U/ml penicillin/streptomycin, 2 mM L-glutamine and 2 µM forskolin (Porter et al., 1986). In order to investigate the influence of forskolin on gene expression, cells were split and cultured in 10% foetal calf serum/DMEM plus forskolin as usual. Prior to the analysis, samples of Schwann cell cultures were incubated for 48 hours in absence of forskolin.

3.2.8 Immunofluorescence

Schwann cells were fixed 20 min in 4% paraformaldehyde in PBS, washed in PBS and blocked in blocking solution (10% donkey serum /0.1% Triton X-100/PBS) for 30 min at room temperature. Cells were incubated overnight with a sheep antibody against CXCL14 diluted 4 µg/ml in blocking solution. The signal was detected with a secondary antibody conjugated to Alexa Fluor® 488 diluted 1:500 in PBS, incubated for 2 hours at room temperature. Slides were mounted in Fluoromont-G. To determine the specificity of the CXCL14 staining, a preabsorption control was carried out (Burry, 2000). Briefly, a 4-fold excess (on a weight basis) of recombinant CXCL14 was preincubated with a sheep antibody against CXCL14 for 1 hour at 37°C. This preincubation mixture was then placed on the slide in place of the primary antibody and the remaining steps were carried out as described above. In each experiment, a slide was done with no primary antibody to confirm that the staining seen was real.

After fixation in 4% formaldehyde in PBS overnight, P30 mice sciatic nerves were dehydrated and embedded in paraffin. 6–8-µm thick transverse sections were cut, deparaffinised and hydrated. Antigen demasking was performed by boiling the sections in PBS for 7 min, followed by 4 boiling steps of 3 min each in citrate buffer 0.1 M pH 6. Sections were then blocked in 10% normal goat serum, for 30 min at room temperature. A rat monoclonal antibody against CXCL14 diluted 5 µg/ml and either a rabbit polyclonal anti-neurofilament (Pan-cocktail) antibody diluted 1:1000, or a rabbit polyclonal antibody against S100 diluted 1:300 were used for immunolabelling (all antibodies were diluted in 10% normal goat serum). The signal was detected by using a secondary antibody conjugated to either Alexa Fluor® 488 or Alexa Fluor® 594 diluted 1:1000 in PBS. Nuclei were stained by using DAPI. Slides were mounted in Fluoromont-G.

For double labelling of CXCL14 with either F4/80-positive macrophages or CD34-positive fibroblasts (Mäurer et al., 2003), fresh frozen cross sections of femoral quadriceps nerve of P30 mice were used. Cryosections were stained with a monoclonal anti-CXCL14 and biotinylated antibodies against F4/80 and CD34, respectively. The CXCL14 staining was visualised by using a secondary antibody conjugated to Alexa 488, while F4/80 and CD34 signals were visualised by Streptavidin Cy3.

3.2.9 Treatment with recombinant CXCL14 (rCXCL14)

80000 cells/well were seeded onto 12-well plates, previously coated with 100 µg/ml poly-D-lysine, and incubated at 37°C with 10% CO₂. The following day, cells were treated with 0, 250, 500, 1000 ng/ml of recombinant CXCL14 and incubated at 37°C, 10% CO₂ for 24 hours. Cells were harvested and RNA was extracted using RNeasy Mini Kit.

3.2.10 Cell proliferation assay

15000 Schwann cells/well were seeded onto 8-well Permanox Lab-Tek Chamber Slides (Nunc, Wiesbaden, Germany), previously coated with 100 µg/ml poly-D-lysine, and incubated at 37°C with 10% CO₂. The following day fresh medium was supplied, supplemented with 0, 250, 500 or 1000 ng/ml of rCXCL14, and incubated for 24 hours at 37°C with 10% CO₂. The following day, bromodeoxyuridine labelling was performed, using 5-bromo-2'-deoxy-uridine Labeling and Detection Kit I and following the manufacturer's protocol. Briefly, cell culture medium was

aspirated and 5-bromo-2'-deoxy-uridine (BrdU) labelling medium was added. Schwann cells were incubated at 37°C, 10% CO₂ for 8 hours. The BrdU labelling medium was aspirated and the chambers were washed three times in washing buffer. Schwann cells were then fixed with the ethanol fixative for at least 20 min at -25°C, then the chambers were washed again for three times in washing buffer. The cells were covered with anti-BrdU working solution and incubated for 30 min at 37°C. The chambers were washed for three times in washing buffer. The cells were covered with anti-mouse-Ig-fluorescein working solution and incubated for 30 min at 37°C. The chambers were washed for three times in washing buffer. To stain Schwann cells' nuclei, cells were covered with DAPI solution for 15 s. Chambers were washed for three times in washing buffer and preparations were covered with Fluoromont-G. DAPI- and BrdU-positive nuclei were counted and the proliferation rate was calculated by the ratio between BrdU- and DAPI-positive nuclei. The proliferation rate of cells treated with different doses of rCXCL14 was calculated as a percentage of the proliferation rate of untreated control cells. The data are represented as the mean value \pm SEM of BrdU+ / DAPI+ cells.

Slides were observed using a Nikon Eclipse TE 200 microscope. Picture acquisition and cell counting were performed using the Lucia 4.21 software.

3.2.11 Plasmid preparation

An amount equal to 1 ng of each vector was transformed into chemically competent *E. coli* cells One Shot TOP10, following the manufacturer's protocol. Bacteria were plated onto LB-agar plates (10 g Bacto-Tryptone, 5 g Bacto-yeast extract, 10 g NaCl, 15 g Bacto-agar, ddH₂O to 1 l. Sterilised

by autoclaving) containing 50 µg/ml ampicillin and grown at 37°C overnight. The presence of the antibiotic ampicillin allowed positive selection of bacterial colonies carrying the vectors.

The following day, pre-cultures of 3 ml of LB (Luria-Bertani medium: 10 g Bacto-Tryptone, 5 g Bacto-yeast extract, 10 g NaCl, ddH₂O to 1 l. Sterilised by autoclaving), prepared by inoculating a single colony for each vector, were grown for about 8 hours at 37°C. A culture of 100 ml LB, prepared by diluting each pre-culture 1:500, was then grown overnight at 37°C, with vigorous shaking. Plasmid DNA was prepared from the bacterial culture, by using EndoFree Plasmid Maxi Kit, following manufacturer's instructions. Briefly, bacterial cells were harvested by centrifugation at 6000 x g for 15 min at 4°C. The bacterial pellet was resuspended in 10 ml Buffer P1, previously supplemented with RNase A. 10 ml Buffer P2 was added, and the suspension was mixed thoroughly by vigorously inverting the tube 4–6 times, then the suspension was incubated at room temperature for 5 min. 10 ml of chilled Buffer P3 was added, then the lysate was mixed immediately and thoroughly by vigorously inverting 4–6 times. The lysate was poured into the barrel of the QIAfilter Cartridge and incubated at room temperature for 10 min. Then, the cap was removed from the QIAfilter Cartridge outlet nozzle and the plunger was inserted gently into the QIAfilter Maxi Cartridge and the cell lysate was filtered into a 50 ml tube. 2.5 ml of Buffer ER was added to the filtered lysate, the lysate was mixed by inverting the tube approximately 10 times and incubated on ice for 30 min. Meanwhile a QIAGEN-tip 500 was equilibrated by applying 10 ml Buffer QBT. The filtered lysate was applied to the QIAGEN-tip and allowed it to enter the resin by gravity flow. The QIAGEN-tip was washed with 2 x 30 ml Buffer QC, then DNA was eluted with 15 ml Buffer QN. DNA was precipitated by adding 10.5 ml (0.7 volumes) room-temperature isopropanol to the eluted DNA. After mixing, the tube was centrifuged immediately at ≥15000 x g for 30 min at 4°C. The supernatant was decanted carefully, DNA pellet was washed with 5 ml of endotoxin-free room-

temperature 70% ethanol and centrifuged at $\geq 15000 \times g$ for 10 min. The supernatant was decanted carefully. The pellet was air-dried for 5–10 min and DNA redissolved in 500 μl of endotoxin-free Buffer TE. DNA concentration was determined by UV spectrophotometry at 260 nm, by using a Nanodrop ND-1000UV/Vis spectrophotometer.

3.2.12 Transfection of Schwann cells

80000 Schwann cells/well were seeded onto 12-well plates, previously coated with 100 $\mu\text{g}/\text{ml}$ poly-D-lysine, and incubated at 37°C with 10% CO₂. The following day, Schwann cells were transfected by using FuGENE HD transfection reagent. Cells were transfected with either a mix of four different vectors containing *Cxcl14*-specific short hairpin RNAs (shRNAs), the H1-*kip2* suppression vector containing a *p57kip2*-specific shRNA, or corresponding control vectors. Vectors expressing *Cxcl14*-specific shRNAs, the control vector containing a non-effective shRNA cassette against the *GFP* gene and the empty vector pRS were purchased from OriGene. The *p57kip2*-suppression vector (H1-*kip2*), as well as the corresponding control vector were used as indicated by Heinen and colleagues (Heinen et al., 2008). Co-transfection with the pcDNA3-hyg-citrine vector containing cDNA encoding Citrine, as well as hygromycin resistance, allowed visualisation and positive selection of transfected cells, respectively (Heinen et al., 2008). A total amount of 0.84 μg vector DNA per well was transfected. The pcDNA3-hyg-citrine vector was one fifth of the total, while four fifth was represented by the vector containing the target sequence (either the *p57kip2*- or the *Cxcl14*-specific shRNAs). In the control wells, the suppression vector was substituted with an empty vector. The following mixture was prepared for each vector combination:

- ❖ 84 μl /well serum free-DMEM + 2.5 μl /well FuGENE HD transfection reagent

and incubated for 10 min. The vectors combinations were prepared in distinct tubes, the mix DMEM/FuGENE HD was added and the transfection mix was incubated for additional 10 min. The Schwann cell medium was changed with fresh complete DMEM. 86-87 μ l of each transfection mix, containing DMEM/FuGENE HD + pcDNA3-hyg-citrine/suppression (control) vector, was added to the cells. The cells were incubated at 37°C with 10% CO₂. Three days after transfection, cells positively transfected were selected by addition of 50 μ g/ml of hygromycin into medium. 4 days post-selection, cells were harvested and RNA was extracted using RNeasy Mini Kit.

3.2.13 RNA extraction

RNA was extracted using two different methods: the TRIzol reagent was used to extract RNA from peripheral nerves, while the RNeasy Mini Kit was used to extract RNA from cultured cells.

Prior to extract RNA using the TRIzol reagent, peripheral nerves were homogenised in 300 μ l of TRIzol reagent, using a Polytron homogeniser. The homogenised samples were then incubated for 5 min at room temperature to permit the complete dissociation of nucleoprotein complexes. 60 μ l (1/5 of the volume of TRIzol reagent used for the initial homogenisation) of chloroform was added to the samples, the tubes were shaken vigorously by hand for 15 s and incubated at room temperature for 2 to 3 min. The samples were centrifuged at 12000 \times g for 15 min at 4°C (Following centrifugation, the mixture separates into a lower red, phenol-chloroform phase, an interphase, and a colorless upper aqueous phase. RNA remains exclusively in the aqueous phase). The aqueous phase was transferred to a fresh tube and the RNA from the aqueous phase was precipitated by mixing with 150 μ l (1/2 of the volume of TRIzol reagent used for the initial homogenisation) of isopropyl alcohol. Samples were incubated at -20°C overnight and then

centrifuged at $12000 \times g$ for 25 minutes at 4°C . The supernatant was removed carefully and the RNA pellet was washed once with 75% ethanol, adding at least $300 \mu\text{l}$ of 75% ethanol per $300 \mu\text{l}$ of TRIzol reagent used for the initial homogenisation. The samples were mixed by vortexing and centrifuged at $7500 \times g$ for 5 min at 4°C . At the end of the procedure, the RNA pellet was air-dried for 5-10 minutes and dissolved in 15-20 μl of RNase-free water.

Extraction with the RNeasy Mini Kit was carried out following manufacturer's directions. Briefly, $350 \mu\text{l}$ of Buffer RLT was used to lysate cells contained in two wells of a 12-well plate (two wells per treatment were pooled). The lysate was collected with a rubber scraper and pipetted into a microcentrifuge tube. The lysate was mixed to ensure that no cell clumps were visible, pipetted directly into a QIAshredder spin column placed in a 2 ml collection tube and centrifuged for 2 min at full speed. One volume of 70% ethanol was added to the homogenised lysate and the mixture was mixed well by pipetting. Up to $700 \mu\text{l}$ of the sample was transferred to an RNeasy spin column placed in a 2 ml collection tube and centrifuged for 20 s at $\geq 8000 \times g$ ($\geq 10000 \text{ rpm}$). The flow-through was discarded. $700 \mu\text{l}$ of Buffer RW1 was added to the RNeasy spin column and the column was centrifuged for 20 s at $\geq 8000 \times g$ ($\geq 10000 \text{ rpm}$) to wash the spin column membrane. The flow-through was discarded. $500 \mu\text{l}$ of Buffer RPE was added to the RNeasy spin column. The column was centrifuged for 20 s at $\geq 8000 \times g$ ($\geq 10000 \text{ rpm}$) to wash the spin column membrane. The flow-through was discarded thereafter. $500 \mu\text{l}$ of Buffer RPE was added to the RNeasy spin column. The column was centrifuged for 2 min at $\geq 8000 \times g$ ($\geq 10000 \text{ rpm}$). The RNeasy spin column was placed in a new 2 ml collection tube and centrifuged at full speed for 1 min. The RNeasy spin column was then placed in a new 1.5 ml collection tube, $30 \mu\text{l}$ RNase-free water was added to the spin column membrane and the column was centrifuged for 1 min at $\geq 8000 \times g$

(≥ 10000 rpm) to elute the RNA. This last step was repeated using the same eluate to elute more RNA in the same collection tube; this ensure a higher RNA concentration.

RNA concentration was determined by UV spectrophotometry at 260 nm, by using a Nanodrop ND-1000UV/Vis spectrophotometer.

3.2.14 Quantitative RT-PCR (qRT-PCR)

An amount of 500 nanograms of total RNA (deriving from three animals of each genotype, for each age) was treated with Deoxyribonuclease I (DNase I). Briefly, 500 ng RNA were mixed with 1 μ l of 1U/ μ l Deoxyribonuclease I, 1 μ l Deoxyribonuclease I Reaction Buffer, LiChrosolv water to 10 μ l, then the mix was incubated 15 min at room temperature. 1 μ l EDTA 25 mM was added and the mix was incubated at 65°C for 10 min, to inactivate the enzyme. The RNA, so treated, was then reverse-transcribed. Briefly, 500 ng of random primers and 3 μ l of 10 mM dNTPs were added to the RNA, the mix was incubated 5 min at 65°C. The following mix was then added to the initial reaction:

	Initial Concentration	Final Concentration	Volume (μ l)
First Strand Buffer	5x	1x	5
DTT	0.1 M	0.01 M	2.5
RNase Out	40 U/ μ l		0.5
Superscript II	200 U/ μ l		1.2
LiChrosolv water to 25 μ l			0.8

The total volume of the reverse-transcription reaction was 25 μ l. The reaction was carried out by incubating 10 min at 25°C, 1 h at 42°C, 15 min at 70°C. At the end of the reaction, the cDNA was diluted 1:6 in LiChrosolv water.

Single PCR reactions of 30 μ l each were prepared for every cDNA. The mix was prepared in the following way:

	Initial Concentration	Final Concentration	Volume (μ l)
Forward primer	5 μ M	0.3 μ M	1.8
Reverse primer	5 μ M	0.3 μ M	1.8
Power SYBR® Green PCR Master Mix	2x	1x	15
LiChrosolv water to 50 μ l			6.4
Template (cDNA)			5
Total Volume			30

All samples were amplified in triplicates by using the 7000 Real-Time PCR System. At the end, a dissociation curve at 60°C was generated to ensure amplification of a single product and absence of primer dimers. Data were acquired using the SDS 2.0 software. Gene expression values, normalised to the expression of the endogenous housekeeping gene *Gapdh* (glyceraldehyde 3-phosphate dehydrogenase), were determined by using the comparative Ct method (see below). Expression levels are expressed as numbers relative to reference's values. Homoscedastic, unpaired, 2-tailed Student's t-test was used to analyse the data and to determine the statistical significance of any difference in gene expression.

Primers (see table below) were designed by using Primer3 software (http://biotools.umassmed.edu/bioapps/primer3_www.cgi) and purchased from Eurofins MWG Operon.

	Forward Primer	Reverse Primer
Rat/Mouse <i>Gapdh</i>	TCATCATCTCCGCCCTTCT	AAGCAGTTGGTGGTGCAGGA
Mouse <i>Cxcl14</i>	GTGTGACTCCACTGTGGCCC	GAAGGACCTGCTCCCAATTG
Rat <i>Cxcl14</i>	GACCCTGCACCCTCTCCTGT	GATTCACAGCCGTCCAGTG
Mouse <i>Nin1</i>	CTGTGTGCAGAGCCCAAGGT	CGGTTCCACATGTCTCAGG
Mouse <i>Tnc</i>	AGAAGGTTTCACGGGCGAAG	AAGCCCTCGTTGCAAACACA
Rat/Mouse <i>Ccnd1</i>	GAGGCGGATGAGAACAAGCA	GGAGGGTGGGTGGAAATGA
Mouse <i>Pmp22</i>	CGCGGTGCTAGTGTTGCTCT	CCAAGGCGGATGTGGTACAG
Rat <i>Pmp22</i>	GCGGAACACTTGACCCTGAA	TCATTTAAACATGTGGCCCCA
Human <i>PMP22</i>	CTCCGCTGAGCAGAACTTGC	CGATCGTGGAGACGAACAGC
Mouse <i>Mbp</i>	GAGACCCTCACAGCGATCCA	CAAGGATGCCCGTGTCTCTG
Rat <i>Mbp</i>	CAATGGACCCGACAGGAAAC	TGGCATCTCCAGCGTGTTT
Mouse <i>Mpz</i>	TGCTGTTGCTGCTGTTGCTC	CTCCCCTTCTCCATGGCACT
Rat <i>Mpz</i>	ACCTTCAAGGAGCGCATCC	GCCATCCTTCCAGCTAGGGT

3.2.15 Comparative Ct Method

The comparative Ct method involves comparing the Ct (cycle threshold) values of the samples of interest with a control or calibrator, such as a non-treated sample or RNA from normal tissue, for instance from wildtype animals. The Ct values of both the calibrator and the samples of interest are normalised to an appropriate endogenous housekeeping gene, for instance the *Gapdh* gene.

The comparative Ct method is also known as the $2^{-\Delta\Delta Ct}$ method, where

$$\Delta\Delta Ct = \Delta Ct_{\text{sample}} - \Delta Ct_{\text{reference}}$$

Here, $\Delta Ct_{\text{sample}}$ is the Ct value for any sample normalised to the endogenous housekeeping gene and $\Delta Ct_{\text{reference}}$ is the Ct value for the calibrator also normalised to the endogenous housekeeping gene.

4. Results

4.1 Myelin gene expression in the sciatic nerve

The mRNA expression of *Pmp22* in murine peripheral nervous system normally starts to increase during the first 10 days after birth, to reach a maximal value at postnatal day 10, which is maintained over the next 10 days (Garbay et al., 2000). In order to establish if myelin gene expression in C61 *PMP22*-overexpressing mice differed from wildtype expression, quantitative RT-PCR was used to analyse sciatic nerve RNA.

As expected, total *Pmp22* expression was higher in transgenic mice than in wildtype littermates, with the highest level of expression at around P4-P7 (Fig. 4A). Surprisingly, also the expression levels of *Mbp* (Fig. 4B) and *Mpz* (Fig. 4C) transcripts were increased by 60-150% in P4 and P7 transgenic mice. At P11, the latter two myelin genes were down-regulated to wildtype levels, whereas *Pmp22* remained elevated. In the cutaneous saphenous nerve of P7 *PMP22*tg mice, the mRNA expression levels of *Mbp* and *Mpz* were, as opposed to *Pmp22*, comparable to wildtype littermates (Fig. 4D).

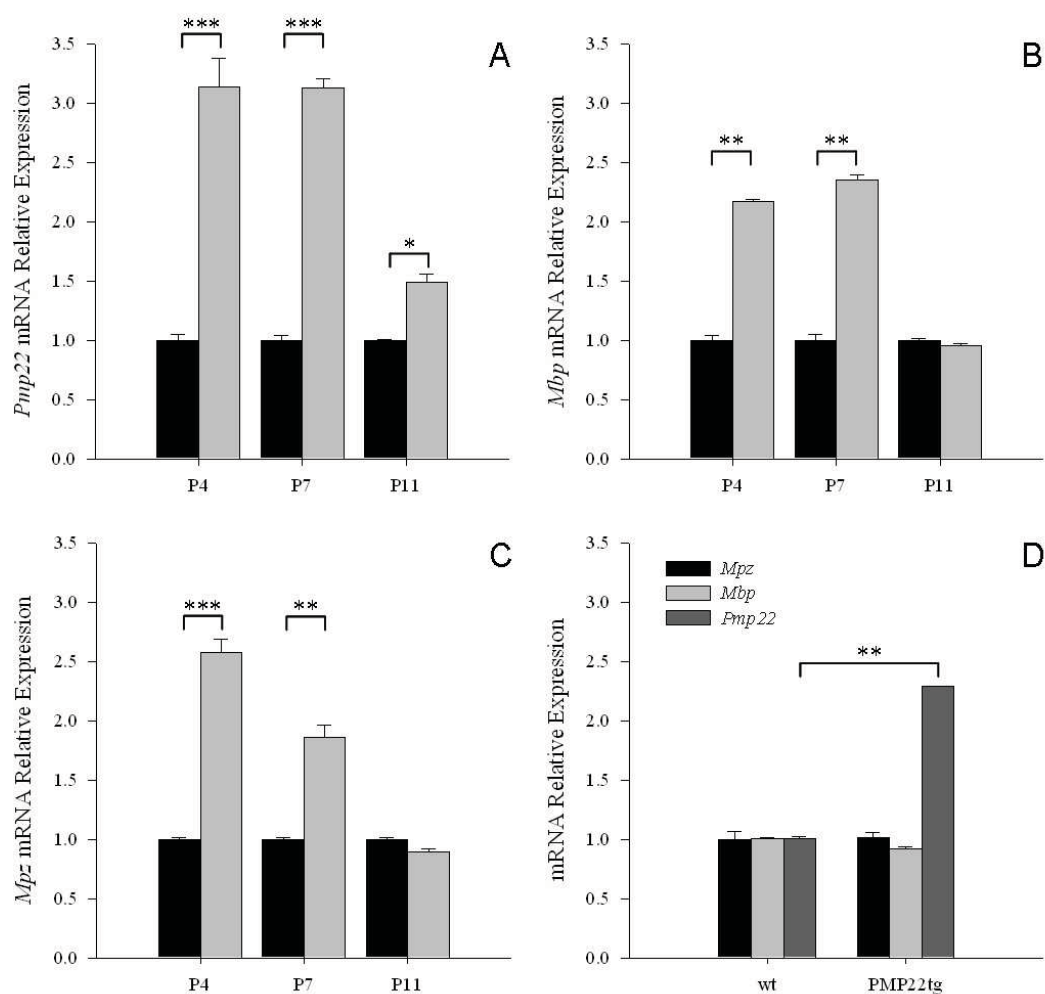
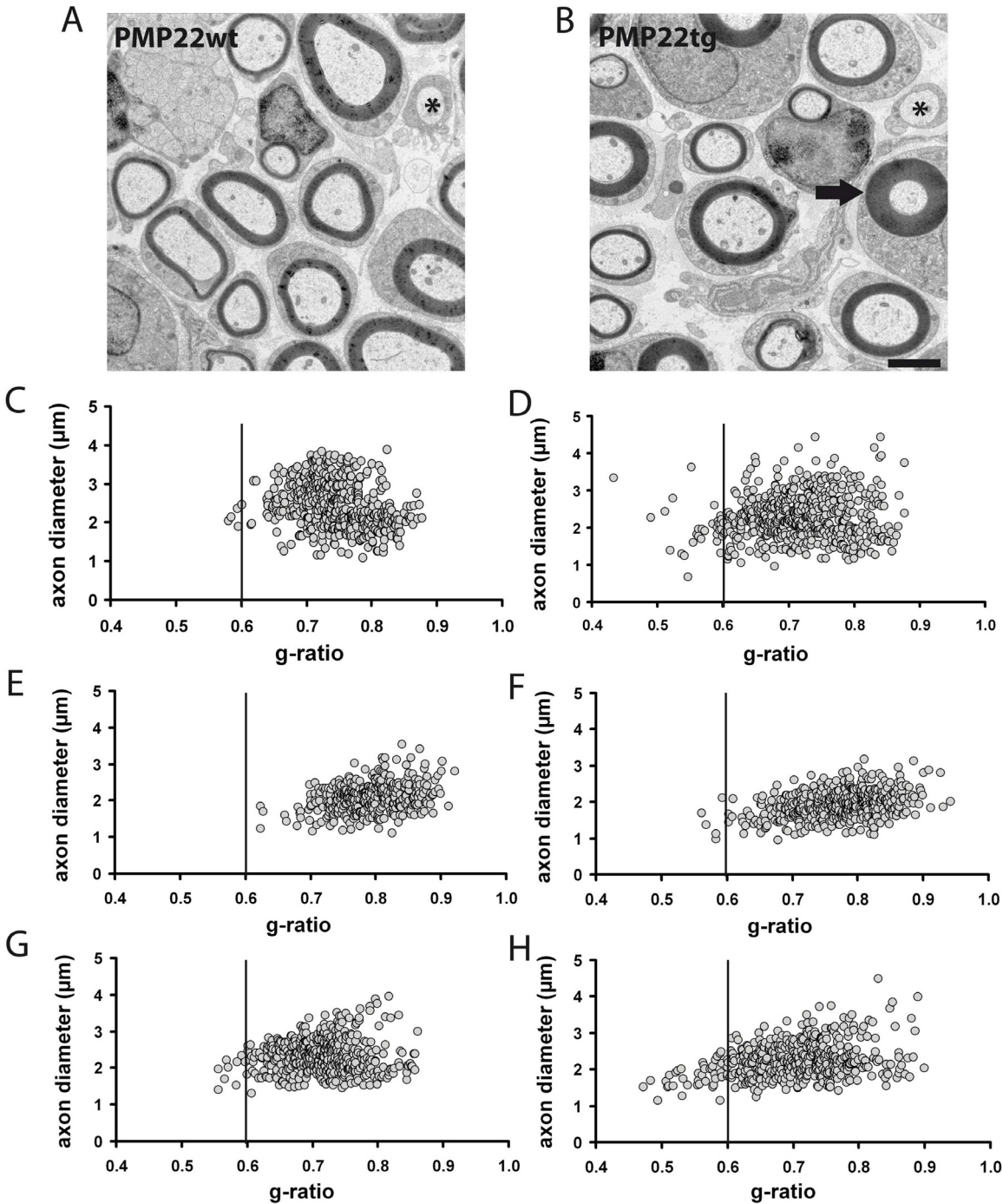


Fig. 4. Expression analysis of *Pmp22* (A), *Mbp* (B) and *Mpz* (C) transcripts by qRT-PCR. Myelin genes were up-regulated in the sciatic nerve of P4 and P7 transgenic mice (grey bars), as compared to wildtype littermates (black bars). At P11, with the exception of *Pmp22*, no significant upregulation was detected. (D): Transcript expression of myelin genes in the cutaneous saphenous nerve at postnatal day 7. Myelin genes, except *Pmp22*, are expressed at equal levels in PMP22tg and wildtype littermates. *Pmp22* mRNA expression in transgenic mice is represented as the sum of human and endogenous *Pmp22* expression levels. * $p < 0.05$; ** $p < 0.001$; *** $p < 0.0001$.

4.2 Morphometric analyses of peripheral nerves

In order to compare qRT-PCR results, which revealed increased mRNA expression of myelin genes in the sciatic nerve of transgenic mice at P4-P7, with nerve morphology, electron microscopy was applied to analyse the peripheral nerves around the same time point. The muscular and cutaneous saphenous branches of the femoral nerve, as well as the sciatic nerve of 7-day-old PMP22tg mice and their wildtype littermates were analysed (Figs. 5A-B). Quantification of correctly sorted and myelinated axons revealed no differences. Accordingly, the percentages of sorted axons devoid of myelin were similar in both genotypes, with 10-12% in the femoral quadriceps nerve, 25-28% in the cutaneous saphenous nerve and 12-15% in the sciatic nerve (data not shown). Furthermore, the axon calibre was not significantly altered in PMP22tg, as compared to wildtype mice, in all peripheral nerves examined (data not shown). However, determination of the g-ratio (axon diameter / total fibre diameter) revealed differences in myelin thickness. In general, a trend towards smaller calibre axons with thicker myelin sheaths was observed in PMP22tg mice, especially in femoral quadriceps nerve and sciatic nerve (Figs. 5C-H). The table in Fig. 5I shows the percentage of axons with a g-ratio lower than 0.6, relative to all investigated axons in the three nerves. These results indicate that femoral quadriceps nerve, sciatic nerve and, to a lesser extent, cutaneous saphenous nerve of P7 PMP22tg mice developed thicker myelin sheaths than corresponding wildtype nerves.



I

	PMP22 wt	PMP22 tg
femoral quadriceps nerve	0.4%	3.8%
cutaneous saphenous nerve	0%	0.7%
sciatic nerve	1.6%	7.6%

(Continues from previous page)

Fig. 5. Morphometric analyses of peripheral nerves of PMP22tg mice and their wildtype littermates at postnatal day 7. (A), (B): Electron micrographs from femoral quadriceps nerve of wildtype (A) and PMP22tg mice (B) (scale bar: 2 μ m). Note the single separated axons, which are not yet surrounded with myelin (asterisk) and hypermyelinated axons (arrow). (C) – (H): Determination of g-ratios in relation to the axonal diameter of wildtype (C, E and G) and PMP22tg mice (D, F and H). PMP22tg mice show a lower g-ratio reflecting thicker myelin sheaths in femoral quadriceps (C, D) and sciatic nerve (G, H), as well as in a lower range in cutaneous saphenous nerve (E, F). (I): The table shows the percentage of axons with a g-ratio lower than 0.6 relative to all investigated axons. In femoral quadriceps and sciatic nerve, PMP22tg mice reveal a higher percentage of thicker myelin sheaths.

These results were obtained in collaboration with Prof. Dr. Rudolf Martini and Bianca Kohl from the Department of Neurology of the University of Würzburg, Germany, who performed the electron microscopy analyses.

4.3 Gene selection and expression study on selected genes

Array hybridisations were performed previously by Dr. Kerstin Hasenpusch-Theil in our laboratory, in order to compare sciatic nerve cDNA expression of wildtype and PMP22tg mice at postnatal day 7. These experiments were carried out by using Affymetrix Gene Chip Mouse Expression Arrays. Data analysis revealed that among the regulated transcripts of annotated genes, 47% were up-regulated while 53% were down-regulated. Amid the down-regulated genes, a predominance encoded proteins involved in lipid metabolic processes. Genes known to be deregulated in CMT1A showed the expected pattern of expression. As previously observed (Giambonini-Brugnoli et al., 2005), genes involved in lipid, steroid and fatty acid biosyntheses were down-regulated. In the list of up-regulated genes some interesting genes were identified, which were selected to confirm the microarray results by qRT-PCR. In order to observe any gene expression variation during nerve development, the expression analyses were extended also to the sciatic nerves of P4 and P11 mice. The genes that were selected for further analyses included cyclin D1 (*Ccnd1*), ninjurin1 (*Ninj1*) and tenascin C (*Tnc*). Additionally, the expression of the gene encoding the α -chemokine CXCL14 (CXC ligand 14) was also analysed, as this gene resulted highly (≥ 3 fold) and significantly up-regulated from the microarray analysis. The qRT-PCR results of the abovementioned genes only partially confirmed the results of the array analysis. In fact, of the three genes *Ccnd1*, *Ninj1* and *Tnc*, only the up-regulation of *Ccnd1* was confirmed at postnatal day 7 in PMP22tg mice (Fig. 6A-C). Nonetheless, a significant up-regulation of all three transcripts was detected at postnatal day 4 in PMP22tg mice, while at P11 none of the three transcripts was significantly up-regulated. Conversely, *Cxcl14* was significantly up-regulated at high level at all stages of development analysed, reaching the highest expression level at P11 (Fig. 6D). Interestingly, *Cxcl14* was well up-

regulated in the sciatic nerve of P7 PMP22tg mice, but not in the saphenous cutaneous nerve of transgenic mice of the same age, where the expression level was comparable to the level observed in wildtype nerves (Fig. 7).

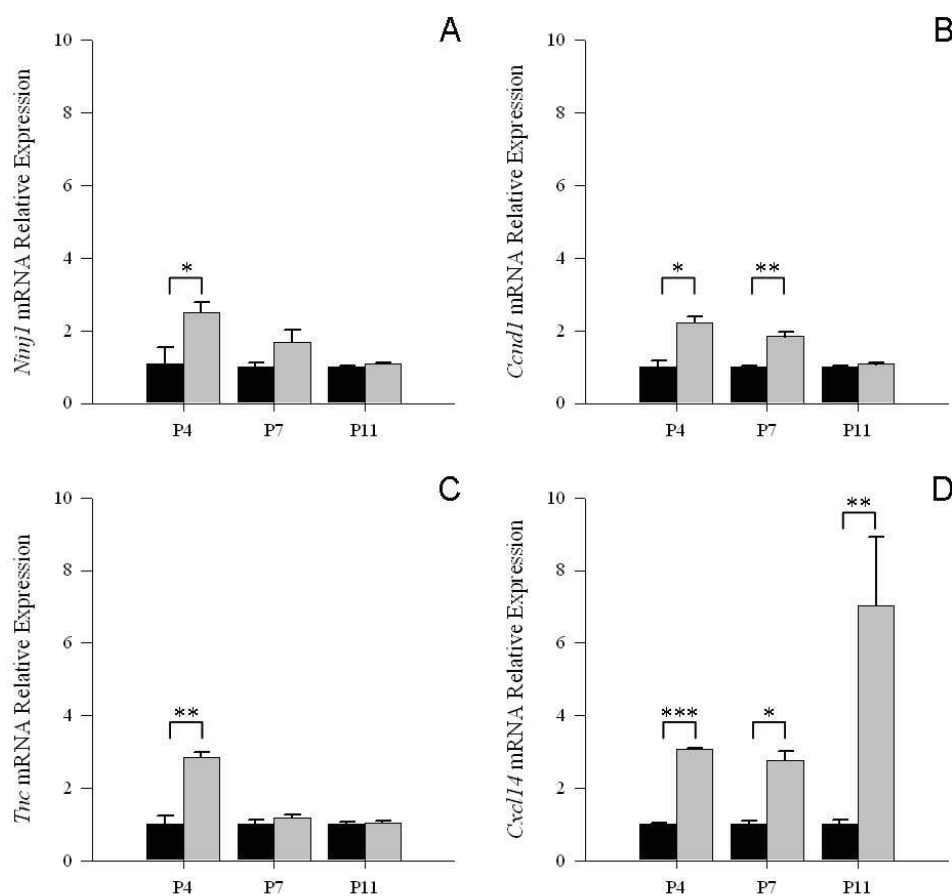


Fig. 6. Expression analysis of *Ninj1* (A), *Ccnd1* (B), *Tnc* (C) and *Cxcl14* (D) transcripts by qRT-PCR. At P4 all the transcripts were significantly up-regulated in PMP22tg mice, as compared to wildtype littermates. In P7 transgenic mice, only *Ccnd1* (B) and *Cxcl14* (D) were significantly up-regulated, while at P11 only *Cxcl14* transcript expression was strongly enhanced in sciatic nerve. Therefore, *Cxcl14* was consistently up-regulated in PMP22tg mice sciatic nerve at all stages of development analysed (D). Black bars: wildtype mice; grey bars: PMP22tg mice. * $p < 0.05$; ** $p < 0.001$; *** $p < 0.0001$.

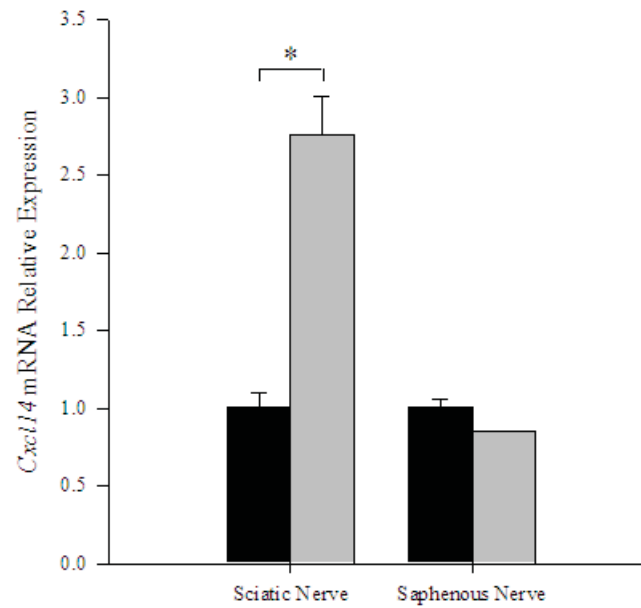


Fig. 7. Comparison between the level of expression of *Cxcl14* in the sciatic and in the saphenous cutaneous nerve of P7 PMP22tg mice. While in P7 transgenic mice *Cxcl14* was highly up-regulated in the sciatic nerve, it was not in the cutaneous nerve. In the cutaneous nerve of transgenic mice the expression level of *Cxcl14* was comparable to the level in wildtype nerves. Black bars: wildtype mice; grey bars: PMP22tg mice. * $p < 0.05$.

4.4 CXCL14 immunodetection in the sciatic nerve of PMP22tg mice

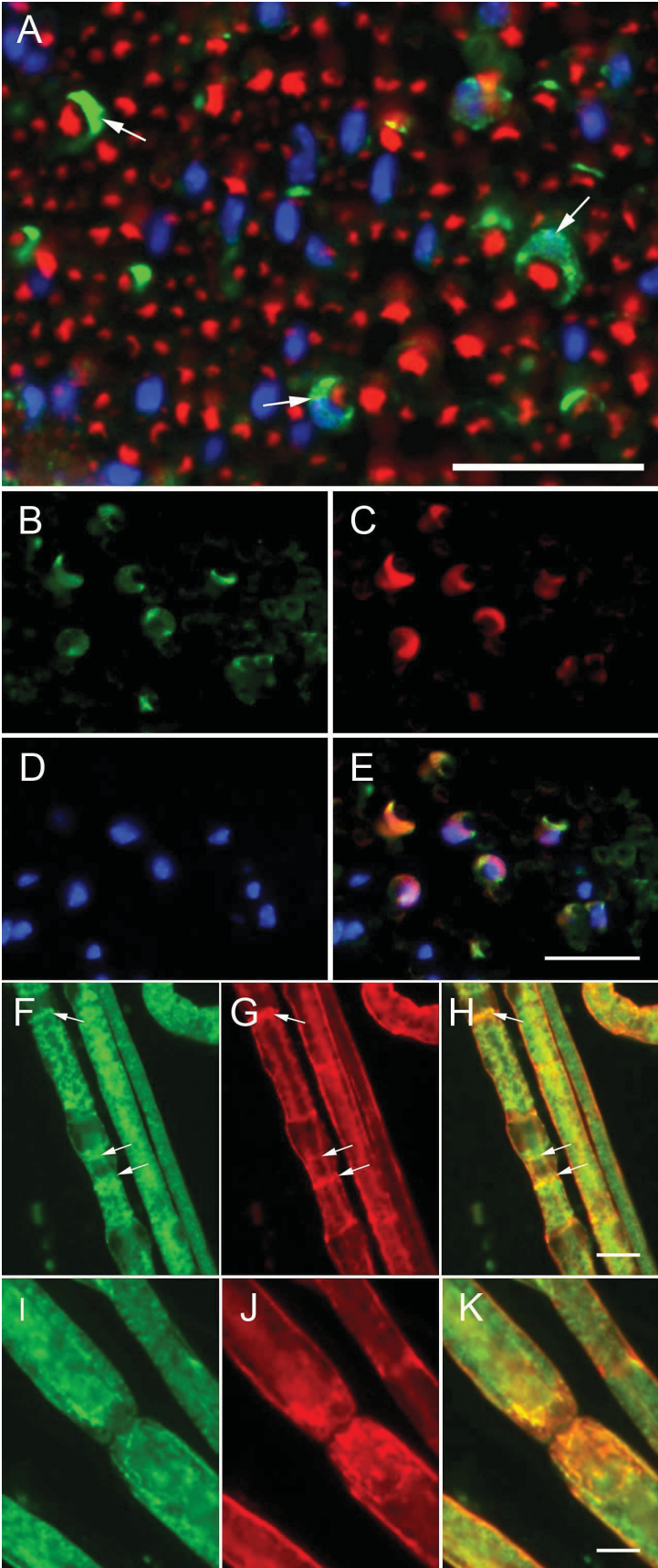
In order to study CXCL14 localisation *in vivo*, immunostaining experiments were carried out on the sciatic nerve. As *Cxcl14* is expressed and up-regulated in PMP22tg animals at least up to postnatal day 30 (data not shown), immunolabelling experiments were carried out on P30 mice, as experimental procedures using teased fibre preparations were easier on older mice.

Immunostaining with a rat monoclonal antibody confirmed that CXCL14 was expressed in sciatic nerve of both wildtype (Fig. 8) and transgenic mice (data not shown). While axons remained immunonegative to CXCL14, as demonstrated by the lack of co-localisation with anti-Pan-neurofilament signal (Fig. 8A), Schwann cells were the main cell type to express the protein (Fig. 8B-D). In Schwann cells, CXCL14 staining was not homogeneously distributed in the cytoplasm, therefore CXCL14 did not completely overlap with S100 signal (Fig. 8E).

Staining of teased-nerve fibre preparations confirmed that CXCL14 was expressed by Schwann cells. CXCL14 immunoreactivity appeared in Schmidt-Lanterman incisures (indicated by arrows) together with S100 (Fig. 8F-H). CXCL14, as S100, was absent from the nodes of Ranvier (Fig. 8I-K).

Schwann cells were the main cell type to express the protein also in the quadriceps nerve, where an exclusive association of CXCL14 with Schwann cells was observed. Conversely, macrophages positive to the extracellular antigen F4/80 (Fig. 9A) and fibroblasts positive to the antigen CD34 (cluster of differentiation 34) (Fig. 9B) did not express the chemokine.

No qualitative differences were observed in the staining of peripheral nerves of wildtype and PMP22tg mice (data not shown).



(Continues from previous page)

Fig. 8. CXCL14 immunodetection in the sciatic nerve. The cross section of the sciatic nerve of a wildtype animal (A) shows that CXCL14 (green) is not localised in the axons, marked by anti-Pan-neurofilament antibody (red), while it is clearly present in the Schwann cells (B), marked by S100 (C). CXCL14 (green) only partially co-localised with S100 (red), as seen in the merged image (E). (F)-(H): Teased-nerve fibre preparation of a sciatic nerve of a wildtype animal. CXCL14 (green) partially co-localised with S100 (red), as seen in (H). Arrows indicate Schmidt-Lantermann incisures. (I)-(K): nodes of Ranvier are neither immunoreactive to CXCL14 nor to S100. Scale bars: 12.5 μm (A), 25 μm (E), 50 μm (H), 25 μm (K).

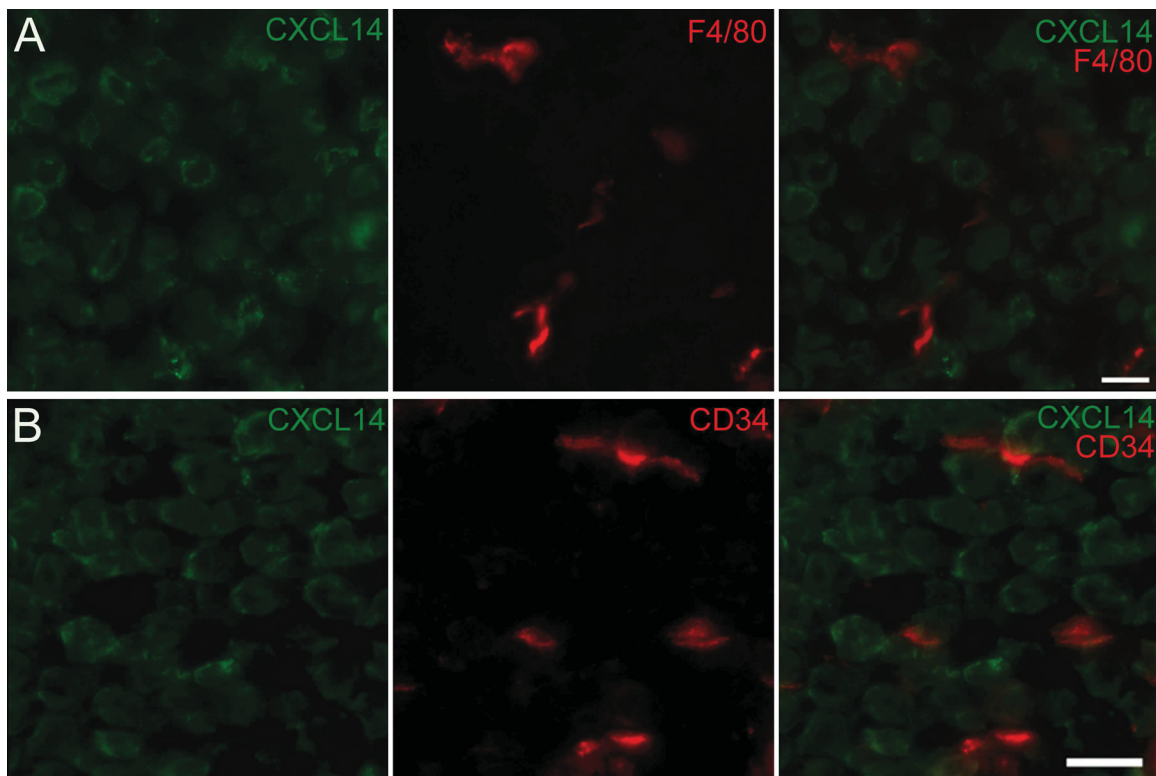


Fig. 9. Double-immunofluorescence using antibodies to CXCL14 and F4/80 (A) and CXCL14 and CD34 (B) on frozen cross sections of quadriceps nerves of wildtype mice. Note that CXCL14 is only associated with Schwann cells (green), but not with macrophages (red in A) or endoneurial fibroblasts (red in B). Scale bar: 10 μ m.

These results were obtained in collaboration with Prof. Dr. Rudolf Martini and Bianca Kohl from the Department of Neurology of the University of Würzburg, Germany.

4.5 *Cxcl14* mRNA expression and CXCL14 immunolocalisation in cultured Schwann cells

Cultured Schwann cells were stained for CXCL14, to confirm the localisation of the chemokine found in this cell type *in vivo*.

Immunostaining experiments confirmed that CXCL14 was expressed also by primary Schwann cells and the signal was exclusively localised in the cytoplasm (Fig. 10A).

Analyses by qRT-PCR showed that *Cxcl14* expression level was considerably increased in Schwann cells treated with forskolin, as compared to non-treated Schwann cells (Fig. 10B). The expression of *Cxcl14* was also explored in cultured Schwann cells, which had been transfected with a *p57kip2*-suppression vector (H1-*kip2*). *p57kip2* is an intrinsic inhibitor of myelinating Schwann cell differentiation, the down-regulation of which is a prerequisite to allow differentiation in the absence of axons (Heinen et al., 2008). Therefore, by suppressing *p57kip2* expression, using shRNA, Schwann cells gradually differentiate. As shown in figure 10C, *Cxcl14* transcript expression steadily increased during *p57kip2* suppression, as Schwann cell differentiation proceeded (Fig. 10C).

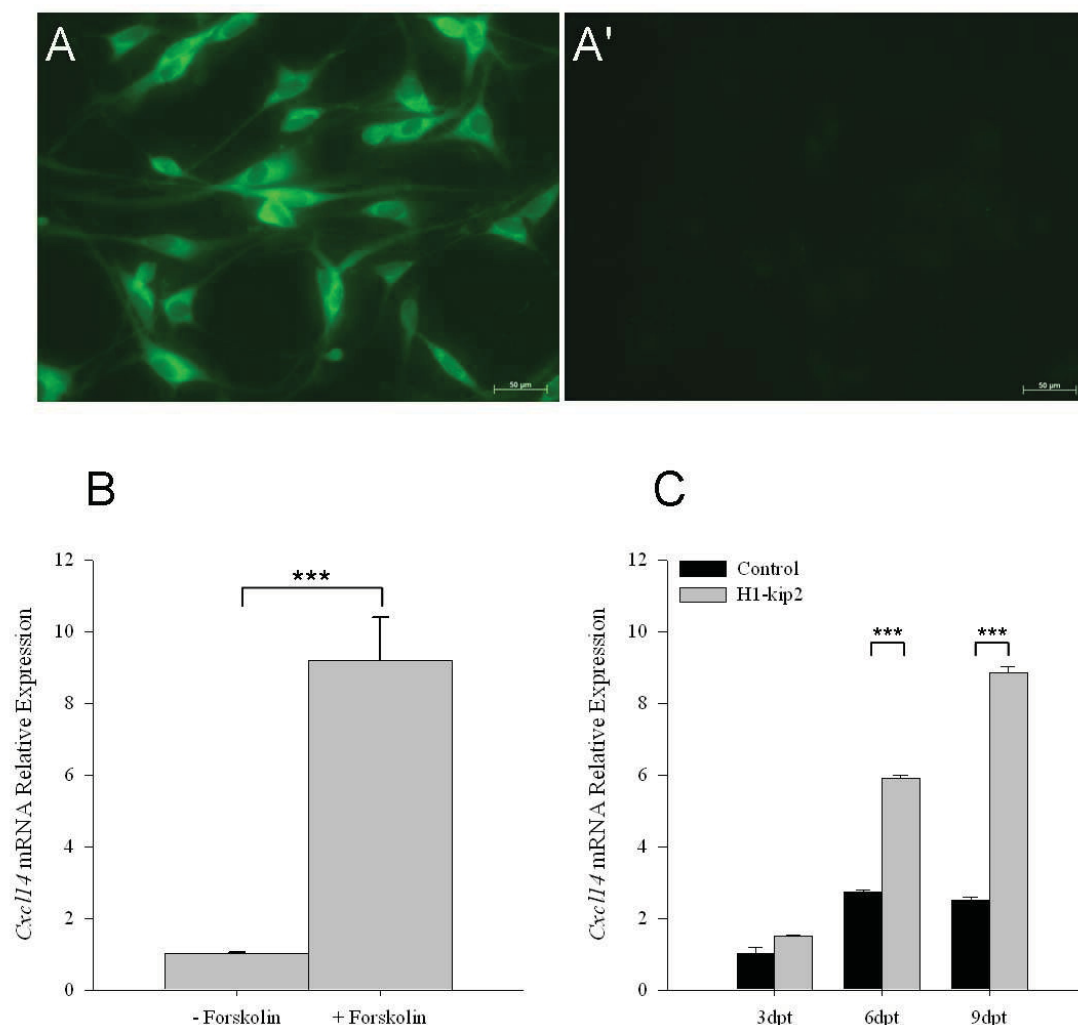


Fig. 10. CXCL14 immunolocalisation and *Cxcl14* mRNA expression in Schwann cells. (A): Anti-CXCL14 immunostaining confirmed that CXCL14 is present in the cytoplasm of cultured Schwann cells. No specific staining was detected when the primary antibody was preincubated with recombinant CXCL14 (A'). (B): Analysis of *Cxcl14* expression in cultured Schwann cells by qRT-PCR. The transcript expression in forskolin-treated Schwann cells was significantly higher than in non-treated Schwann cells. (C) Analysis of *Cxcl14* expression in Schwann cells transfected with the H1-kip2 vector. *Cxcl14* mRNA expression was steadily up-regulated in *p57kip2*-suppressed cells, as opposed to control transfected cells. Nine days after transfection (9 dpt), *Cxcl14* expression was 5 to 9 times higher in suppressed cells than in cells transfected with a control vector. One representative experiment of three is shown. *** $p < 0.0001$.

4.6 Effect of rCXCL14 treatment on Schwann cells

Expression analyses showed that *Cxcl14* is increased in differentiating Schwann cells. The next step was to establish whether the chemokine itself had a direct effect on the Schwann cells. Therefore, Schwann cells were treated with recombinant CXCL14, and the effects on cell cycle and myelin gene expression were analysed.

The proliferation rates of cultured Schwann cells treated with increasing doses of recombinant CXCL14 were determined by detection of DNA-incorporated 5-Bromo-2'-deoxy-uridine. As shown in figure 11, recombinant CXCL14 reduced the rate of Schwann cell proliferation in a dose-dependent manner, when compared to untreated cells. Statistically significant decreases of 13% and 20% were observed at the doses of 500 ng/ml and 1000 ng/ml, respectively. A dose of 250 ng/ml did not affect proliferation (Fig. 11A).

Quantitative RT-PCR analyses revealed that incubation of Schwann cells with rCXCL14 led to a statistically significant increase in the expression of *Mpz*, *Pmp22* and *Mbp*, at a dose of 500 ng/ml (Fig. 11B), while no statistically significant alteration in myelin gene expression was observed when Schwann cells were treated with either 250 or 1000 ng/ml of recombinant CXCL14.

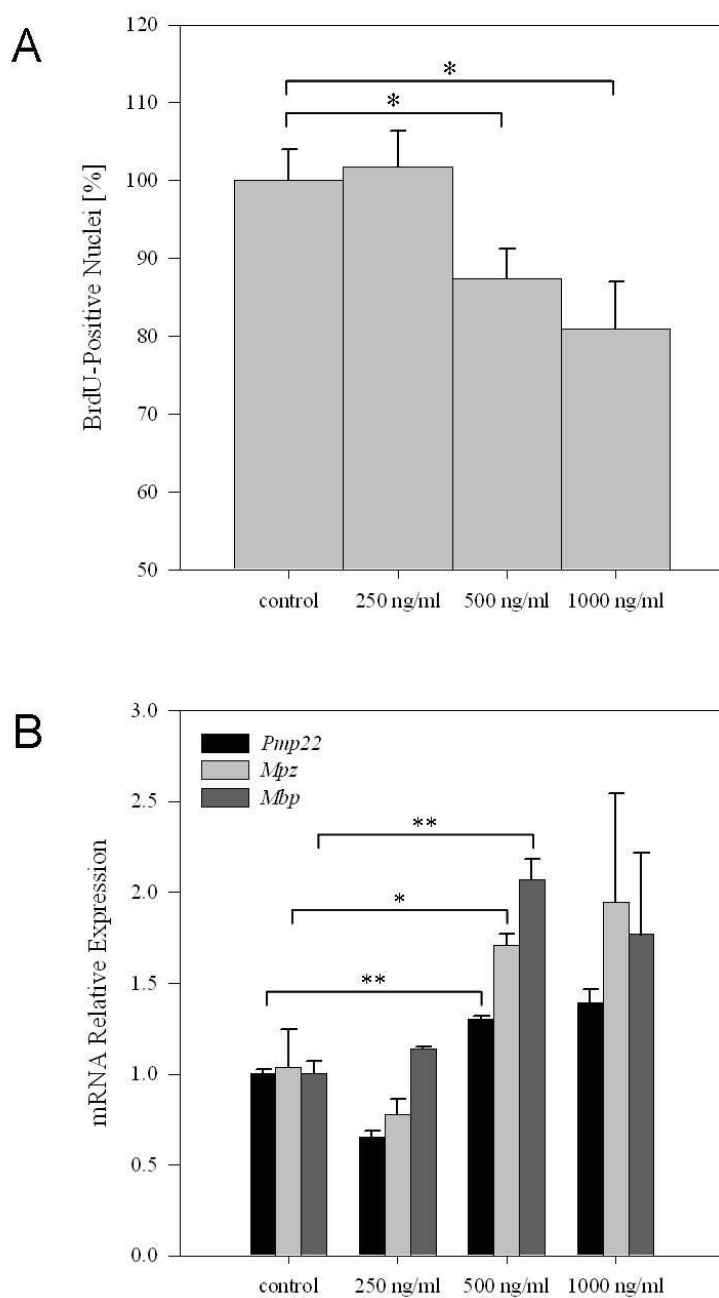


Fig. 11. Schwann cell treatment with recombinant CXCL14. (A) Effect of rCXCL14 on Schwann cell proliferation is analysed by counting BrdU-positive nuclei. Treatment with 500 and 1000 ng/ml of rCXCL14 for 24 hours decreased cell proliferation by 13-20%, respectively. Each bar represents the mean of three independent experiments with SEM as indicated. (B) Effect of 24-hours treatment on myelin gene expression, as analysed by qRT-PCR. Although a dose-dependent increase in the mRNA expression of *Mpz*, *Pmp22* and *Mbp* is apparent, a statistically significant increase was observed only with 500 ng/ml rCXCL14. * $p < 0.05$; ** $p < 0.001$.

4.7 Silencing of *Cxcl14* mRNA expression in Schwann cells

As proven by the treatment of Schwann cells with the recombinant chemokine, CXCL14 is able to induce myelin gene expression. To investigate whether the silencing of *Cxcl14* also affects myelin gene expression, a gene suppression approach was used.

Schwann cells were transfected with either *Cxcl14*-specific short hairpin RNAs, with a control shRNA or with an empty vector. Four days after hygromycin selection, RNA was extracted and gene expression analysed. In three independent experiments, *Cxcl14* mRNA expression was decreased by 80-89%. Along with a decrease in *Cxcl14* expression, the expression levels of *Pmp22* and *Mpz* were also strongly diminished (about 70%). Whereas *Mbp* expression was decreased to a much lesser extent (Fig. 12).

No significant effect on either *Cxcl14* or myelin gene expression was observed when the cells were transfected with a vector containing a non-effective shRNA cassette against the *GFP* gene (data not shown).

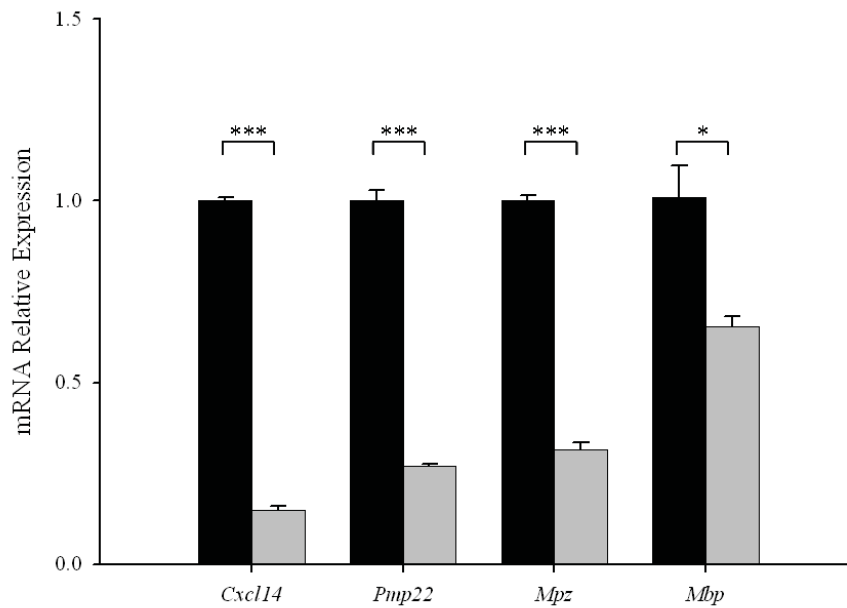


Fig. 12. Effect of suppression of *Cxcl14* on the expression of myelin genes in Schwann cells. In Schwann cells transfected with *Cxcl14*-specific shRNAs, qRT-PCR revealed that *Cxcl14* expression was down-regulated by about 80-89%. *Pmp22*, *Mpz* and to a much lesser extent *Mbp*, were also expressed at significantly lower levels in suppressed Schwann cells, as opposed to control cells. One representative experiment of three is shown. Black bars: control cells; grey bars: *Cxcl14*-suppressed Schwann cells. * $p < 0.05$; *** $p < 0.0001$.

4.8 *Cxcl14* mRNA expression in other models of demyelinating inherited neuropathies

In order to establish if the up-regulation of *Cxcl14* mRNA expression was an exclusive phenomenon of the C61 mouse model, the expression of *Cxcl14* was investigated in two other mouse models of demyelinating forms of inherited neuropathies: the P0^{+/-} mice and Cx32^{-/-} mice. The P0^{+/-} mice express half of the normal dose of P0, while the Cx32^{-/-} mice are completely deficient in the gap-junction protein connexin (Cx) 32. These two models mimic CMT type 1B and CMT type 1X, respectively.

Quantitative RT-PCR analyses carried out at postnatal day 7 revealed that *Cxcl14* was also significantly increased in the sciatic nerve of both animal models, as compared to wildtype animals (Fig. 13).

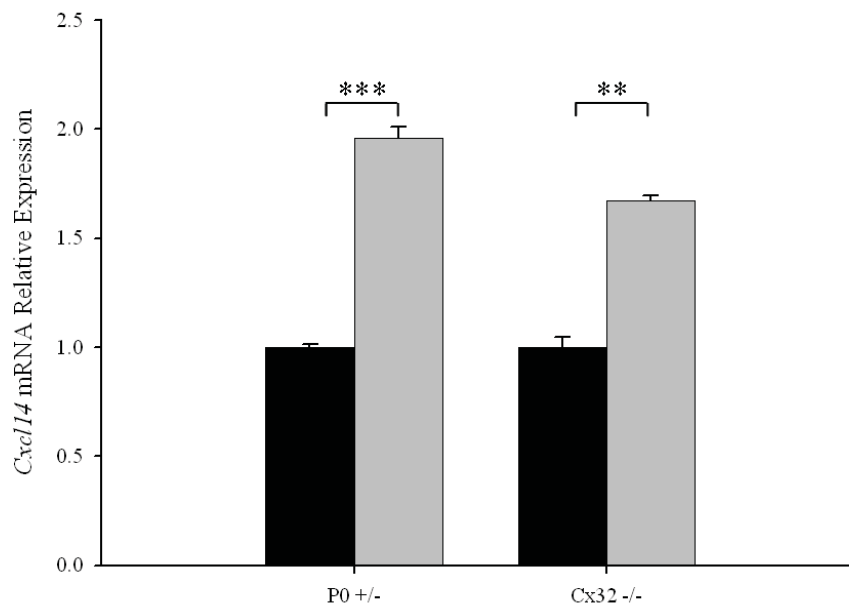


Fig. 13. qRT-PCR analysis of *Cxcl14* expression in P0^{+/-} and Cx32^{-/-} mice, which mimic CMT type 1B and CMT type 1X, respectively. At postnatal day 7 *Cxcl14* is significantly up-regulated (grey bars) in both mutant mouse lines, as compared to wildtype animals (black bars). ** $p < 0.001$; *** $p < 0.0001$.

5. Discussion

In spite of several previous studies, the functional role of PMP22, as well as the mechanisms of myelin degeneration caused by PMP22-overexpression in CMT1A are still unclear. Amongst the several animal models expressing altered levels of PMP22 that were generated, the mouse mutant C61 (Huxley et al., 1996) was chosen for this study. In fact, the mouse model C61 is thought to be an optimal model, as it showed mild *PMP22* over-expression and histopathological features similar to those seen in CMT1A patients. Analyses carried out early in development, at postnatal day 7, showed decreased g-ratio values reflecting thicker myelin sheaths, mainly in the femoral quadriceps and sciatic nerve of C61 mice. This finding, together with the increased myelin gene expression, led to the identification of genes putatively involved in early hypermyelination. Amongst the genes deregulated at P7, the gene encoding the α -chemokine CXCL14 is up-regulated in the sciatic nerve of C61 mice and is highly expressed in Schwann cells triggered to differentiate. Moreover, the treatment with recombinant CXCL14 results in reduced Schwann cell proliferation and in enhanced myelin gene expression. Taken together these data suggest that CXCL14 is involved in *in vitro* Schwann cell differentiation and is a putative marker of Schwann cell myelination/remyelination *in vivo*.

It is established that PMP22 does not function in the initial ensheathment and separation of axons in C61 mice. In fact, while in another PMP22-overexpressing mouse mutant (C22) a lower proportion of single ensheathed myelinated fibres were detected, the C61 mice did not differ significantly from the wildtype controls with regard to the percentage of myelinated fibres at P4 and P10-12 (Robertson et al., 1999). The morphological findings reported in this study concord with these observations, as in the peripheral nerves of C61 mice no relevant alteration in the axon-Schwann

cell relationship was detected at early time points. Nevertheless, at postnatal day 7 decreased g-ratio values were observed in the sciatic nerve, femoral quadriceps nerve and, to a lesser extent, in the cutaneous saphenous nerve of C61 mice. In agreement with enhanced thickness of the myelin sheath of appropriately segregated axons, *Mpz* and *Mbp* mRNA levels were increased in the sciatic nerve of transgenic mice. As expected, the total mRNA expression of *Pmp22* was also increased in the sciatic nerve of transgenic mice at P4, P7 and, to a lesser extent, at P11. Hypermyelinated fibres were previously described in CMT1A-patients (Gabreels-Festen et al., 1995), in the *Pmp22*-overexpressing rat (Sereda et al., 1996), as well as in adult PMP22-transgenic C61 mice (Kobsar et al., 2005). In this study it was shown that thickened myelin sheath can be observed in C61 mice also at very young age (postnatal day 7).

Comparison of the transcriptomes of PMP22tg and wildtype mice, at postnatal day 7 demonstrated that, amongst the down-regulated genes, a predominance encoded proteins involved in lipid biosynthesis and metabolism. Down-regulation of genes involved in lipid biosynthesis was observed also in other *PMP22*-overexpressing animal models (Giambonini-Brugnoli et al., 2005; Vigo et al., 2005). Relevance of lipid and specifically of cholesterol biosynthesis during myelination has been previously proven by several studies (Nagarajan et al., 2002; Verheijen et al., 2003; Wagner-Recio et al., 1991). It is now well established that a steady-state turnover of lipids is required for the maintenance of myelin membrane (Garbay et al., 2000). More recently, Liang and colleagues observed that local *de novo* biosynthesis of fatty acids may play a major role in lipid turnover during periods of active myelination (Liang et al., 2007).

Among the up-regulated genes, cyclin D1, ninjurin1 and tenascin C, as well as the gene encoding the α -chemokine CXCL14 were identified. The identification of ninjurin1 and tenascin C was quite unexpected, as these two genes had been previously identified as up-regulated in the distal stump of

post-injured sciatic nerve (Kubo et al., 2002). In fact, even though axonal degeneration plays a role in causing the clinical disability in CMT1A, no axonal degeneration was observed in the C61 mice at such an early age. Increased expression of the extracellular matrix molecule tenascin C has been found to be indicative of degenerative events in lesioned peripheral nerves (Fruttiger et al., 1995b; Martini et al., 1990). However, up-regulation of tenascin C has been also observed in the sciatic nerve of a myelin-associated glycoprotein (MAG) deficient mouse mutant, possibly reflecting lesion-related events in this myelin mutant (Fruttiger et al., 1995a). Cyclin D1 was up-regulated also in *Pmp22*-overexpressing rats (Atanasoski et al., 2002; Vigo et al., 2005). Myelinating Schwann cells express cyclin D1 in the perinuclear region, but this gene is strongly up-regulated in parallel with Schwann cell proliferation when axons are injured (Atanasoski et al., 2001). Results on Schwann cell proliferation in CMT1A are contrasting though, as *in vitro* experiments on PMP22-overexpressing human Schwann cells from CMT1A patients showed a decreased rate of proliferation (Hanemann et al., 1997). The latter observation was in agreement with a hypothesis suggested previously, which proposed decreased Schwann cell proliferation as an effect of *PMP22*-overexpression, given its homology with the growth arrest-specific gene 3 (*Gas3*) (Spreyer et al., 1991).

Cxcl14 was the most strongly up-regulated gene in the sciatic nerve of C61 mutant mice, identified by the microarray analysis carried out in our laboratory. Subsequent qRT-PCR analyses confirmed that *Cxcl14* was up-regulated at high level in the sciatic nerve of transgenic mice, at all ages examined in this study. CXCL14 is a member of the CXC chemokine family (Hromas et al., 1999), but its function is poorly understood and its receptor still remains unidentified. CXCL14 has been reported to be expressed in normal non-lymphoid tissues and both mouse and human genes are expressed in brain and muscle (Sleeman et al., 2000), and in dermal fibroblasts (Kurth et al., 2001).

In peripheral nerve, an exclusive association of CXCL14 with Schwann cells was observed, while endoneurial fibroblasts and macrophages did not express the chemokine. Immunostaining of cultured Schwann cells confirmed that CXCL14 was expressed also *in vitro*. Analyses by qRT-PCR showed that *Cxcl14* expression level was considerably increased in Schwann cells treated with forskolin and in cells in which the *p57kip2* gene had been suppressed. Forskolin is known to directly activate cAMP pathways and to mimic the initial steps of myelination (Morgan et al., 1991). While *p57kip2* has recently been identified as an intrinsic inhibitor of myelinating Schwann cell differentiation, the down-regulation of which is a prerequisite to allow Schwann cell differentiation in absence of axons (Heinen et al., 2008). These findings suggest that CXCL14 could be involved in Schwann cell differentiation. The result of Schwann cell treatment with recombinant CXCL14 is in agreement with this observation, as increasing doses of the chemokine reduced cell proliferation and up-regulation of the myelin genes. Interestingly, increased expression of the myelin genes was reported also in the sciatic nerve of PMP22tg mice around postnatal days 4-7. Although a correspondence between the normal expression of *Cxcl14* and the myelin genes in the cutaneous nerve of PMP22tg mice was observed, the increased expression of myelin genes in the sciatic nerve at P4-P7 does not mirror the profile of *Cxcl14*, which is up-regulated in the sciatic nerve up to postnatal day 30. The lack of correlation between the timing of *Cxcl14* and myelin gene over-expression *in vivo* might depend on the complex environment, in which several factors contribute to regulate myelin gene expression during myelination and remyelination (Ghislain and Charnay, 2006; Jessen and Mirsky, 2005). On the other hand, silencing of *Cxcl14* expression in the present study demonstrated that CXCL14 is certainly involved in myelin gene expression enhancement in cultured Schwann cells. A putative role for CXCL14 as factor involved in myelin gene expression and as marker of myelination/remyelination is confirmed by its up-regulation at

postnatal day 7 in the sciatic nerve of other mouse models of inherited neuropathies, such as P0^{+/-} and Cx32 ^{-/-} mouse lines, which are animal models of CMT type 1B and CMT type 1X, respectively. An almost normal myelin formation is observed in both models during the first months of life, which is followed by a slowly progressing demyelinating neuropathy. Moreover, in both models there is a substantial increase of CD8⁺ T-lymphocytes and macrophages within the demyelinating nerves and the inactivation of either cell type leads to a substantial alleviation of the demyelinating phenotype (Ip et al., 2006). Recent studies have laid particular focus on the role of another chemokine, MCP-1 (monocyte chemoattractant protein-1, also known as CCL2). This factor is up-regulated in mutant Schwann cells, mediates macrophage immigration into peripheral nerves and is involved in demyelination, as reflected by an ameliorated phenotype when MCP-1 is reduced (Ip et al., 2006). Interestingly, MCP-1 is also upregulated in the PMP22-C61 mutant, suggesting a similar role during demyelination (Kobsar et al., 2005). However, further studies are needed to disclose the functional relevance of both CXCL14 and MCP-1 with regard to their pathogenetic impact on the CMT1A model.

6. References

- Agostoni, E., Gobessi, S., Brancolini, C., Schneider, C., 1999. Identification and characterization of a new member of the gas3/PMP22 gene family in *C. elegans*. *Gene* 234, 267-274.
- Atanasoski, S., Scherer, S.S., Nave, K.A., Suter, U., 2002. Proliferation of Schwann cells and regulation of cyclin D1 expression in an animal model of Charcot-Marie-Tooth disease type 1A. *J Neurosci Res* 67, 443-449.
- Atanasoski, S., Shumas, S., Dickson, C., Scherer, S.S., Suter, U., 2001. Differential cyclin D1 requirements of proliferating Schwann cells during development and after injury. *Mol Cell Neurosci* 18, 581-592.
- Baechner, D., Liehr, T., Hameister, H., Altenberger, H., Grehl, H., Suter, U., Rautenstrauss, B., 1995. Widespread expression of the peripheral myelin protein-22 gene (PMP22) in neural and non-neural tissues during murine development. *J Neurosci Res* 42, 733-741.
- Berciano, J., Garcia, A., Combarros, O., 2003. Initial semeiology in children with Charcot-Marie-Tooth disease 1A duplication. *Muscle Nerve* 27, 34-39.
- Berger, P., Young, P., Suter, U., 2002. Molecular cell biology of Charcot-Marie-Tooth disease. *Neurogenetics* 4, 1-15.
- Berghoff, M., Samsam, M., Muller, M., Kobsar, I., Toyka, K.V., Kiefer, R., Mäurer, M., Martini, R., 2005. Neuroprotective effect of the immune system in a mouse model of severe dysmyelinating hereditary neuropathy: enhanced axonal degeneration following disruption of the RAG-1 gene. *Mol Cell Neurosci* 28, 118-127.
- Bosse, F., Brodbeck, J., Müller, H.W., 1999. Post-transcriptional regulation of the peripheral myelin protein gene PMP22/gas3. *J Neurosci Res* 55, 164-177.

- Brookes, J.P., Fields, K.L., Raff, M.C., 1979. Studies on cultured rat Schwann cells. I. Establishment of purified populations from cultures of peripheral nerve. *Brain Res* 165, 105-118.
- Burry, R.W., 2000. Specificity controls for immunocytochemical methods. *J Histochem Cytochem* 48, 163-166.
- Carenini, S., Maurer, M., Werner, A., Blazyca, H., Toyka, K.V., Schmid, C.D., Raivich, G., Martini, R., 2001. The role of macrophages in demyelinating peripheral nervous system of mice heterozygously deficient in p0. *J Cell Biol* 152, 301-308.
- Chance, P.F., Alderson, M.K., Leppig, K.A., Lensch, M.W., Matsunami, N., Smith, B., Swanson, P.D., Odelberg, S.J., Distèche, C.M., Bird, T.D., 1993. DNA deletion associated with hereditary neuropathy with liability to pressure palsies. *Cell* 72, 143-151.
- Cicarelli, C., Philipson, L., Sorrentino, V., 1990. Regulation of expression of growth arrest-specific genes in mouse fibroblasts. *Mol Cell Biol* 10, 1525-1529.
- D'Urso, D., Brophy, P.J., Staugaitis, S.M., Gillespie, C.S., Frey, A.B., Stempak, J.G., Colman, D.R., 1990. Protein zero of peripheral nerve myelin: biosynthesis, membrane insertion, and evidence for homotypic interaction. *Neuron* 4, 449-460.
- D'Urso, D., Ehrhardt, P., Müller, H.W., 1999. Peripheral myelin protein 22 and protein zero: a novel association in peripheral nervous system myelin. *J Neurosci* 19, 3396-3403.
- D'Urso, D., Müller, H.W., 1997. Ins and outs of peripheral myelin protein-22: mapping transmembrane topology and intracellular sorting. *J Neurosci Res* 49, 551-562.
- De Leon, M., Nahin, R.L., Mendoza, M.E., Ruda, M.A., 1994. SR13/PMP-22 expression in rat nervous system, in PC12 cells, and C6 glial cell lines. *J Neurosci Res* 38, 167-181.

- De Leon, M., Welcher, A.A., Suter, U., Shooter, E.M., 1991. Identification of transcriptionally regulated genes after sciatic nerve injury. *J Neurosci Res* 29, 437-448.
- Desarnaud, F., Bidichandani, S., Patel, P.I., Baulieu, E.E., Schumacher, M., 2000. Glucocorticosteroids stimulate the activity of the promoters of peripheral myelin protein-22 and protein zero genes in Schwann cells. *Brain Res* 865, 12-16.
- Desarnaud, F., Do Thi, A.N., Brown, A.M., Lemke, G., Suter, U., Baulieu, E.E., Schumacher, M., 1998. Progesterone stimulates the activity of the promoters of peripheral myelin protein-22 and protein zero genes in Schwann cells. *J Neurochem* 71, 1765-1768.
- Dickson, K.M., Bergeron, J.J., Shames, I., Colby, J., Nguyen, D.T., Chevet, E., Thomas, D.Y., Snipes, G.J., 2002. Association of calnexin with mutant peripheral myelin protein-22 ex vivo: a basis for "gain-of-function" ER diseases. *Proc Natl Acad Sci U S A* 99, 9852-9857.
- Erne, B., Sansano, S., Frank, M., Schaeren-Wiemers, N., 2002. Rafts in adult peripheral nerve myelin contain major structural myelin proteins and myelin and lymphocyte protein (MAL) and CD59 as specific markers. *J Neurochem* 82, 550-562.
- Filbin, M.T., Walsh, F.S., Trapp, B.D., Pizzey, J.A., Tennekoon, G.I., 1990. Role of myelin P0 protein as a homophilic adhesion molecule. *Nature* 344, 871-872.
- Fleming, J.V., Fontanier, N., Harries, D.N., Rees, W.D., 1997. The growth arrest genes *gas5*, *gas6*, and *CHOP-10 (gadd153)* are expressed in the mouse preimplantation embryo. *Mol Reprod Dev* 48, 310-316.
- Fruttiger, M., Montag, D., Schachner, M., Martini, R., 1995a. Crucial role for the myelin-associated glycoprotein in the maintenance of axon-myelin integrity. *Eur J Neurosci* 7, 511-515.

- Fruttiger, M., Schachner, M., Martini, R., 1995b. Tenascin-C expression during wallerian degeneration in C57BL/Wlds mice: possible implications for axonal regeneration. *J Neurocytol* 24, 1-14.
- Gabreels-Festen, A.A., Bolhuis, P.A., Hoogendijk, J.E., Valentijn, L.J., Eshuis, E.J., Gabreels, F.J., 1995. Charcot-Marie-Tooth disease type 1A: morphological phenotype of the 17p duplication versus PMP22 point mutations. *Acta Neuropathol* 90, 645-649.
- Gabreels-Festen, A.A., Hoogendijk, J.E., Meijerink, P.H., Gabreels, F.J., Bolhuis, P.A., van Beersum, S., Kulkens, T., Nelis, E., Jennekens, F.G., de Visser, M., van Engelen, B.G., Van Broeckhoven, C., Mariman, E.C., 1996. Two divergent types of nerve pathology in patients with different P0 mutations in Charcot-Marie-Tooth disease. *Neurology* 47, 761-765.
- Garbay, B., Heape, A.M., Sargueil, F., Cassagne, C., 2000. Myelin synthesis in the peripheral nervous system. *Prog Neurobiol* 61, 267-304.
- Ghislain, J., Charnay, P., 2006. Control of myelination in Schwann cells: a Krox20 cis-regulatory element integrates Oct6, Brn2 and Sox10 activities. *EMBO Rep* 7, 52-58.
- Giambonini-Brugnoli, G., Buchstaller, J., Sommer, L., Suter, U., Mantei, N., 2005. Distinct disease mechanisms in peripheral neuropathies due to altered peripheral myelin protein 22 gene dosage or a Pmp22 point mutation. *Neurobiol Dis* 18, 656-668.
- Giese, K.P., Martini, R., Lemke, G., Soriano, P., Schachner, M., 1992. Mouse P0 gene disruption leads to hypomyelination, abnormal expression of recognition molecules, and degeneration of myelin and axons. *Cell* 71, 565-576.
- Grandis, M., Leandri, M., Vigo, T., Cilli, M., Sereda, M.W., Gherardi, G., Benedetti, L., Mancardi, G., Abbruzzese, M., Nave, K.A., Nobbio, L., Schenone, A., 2004. Early abnormalities in

sciatic nerve function and structure in a rat model of Charcot-Marie-Tooth type 1A disease.

Exp Neurol 190, 213-223.

Greenfield, S., Brostoff, S., Eylar, E.H., Morell, P., 1973. Protein composition of myelin of the peripheral nervous system. J Neurochem 20, 1207-1216.

Hagedorn, L., Suter, U., Sommer, L., 1999. P0 and PMP22 mark a multipotent neural crest-derived cell type that displays community effects in response to TGF-beta family factors.

Development 126, 3781-3794.

Hahn, A.F., Ainsworth, P.J., Bolton, C.F., Bilbao, J.M., Vallat, J.M., 2001. Pathological findings in the x-linked form of Charcot-Marie-Tooth disease: a morphometric and ultrastructural analysis. Acta Neuropathol 101, 129-139.

Hai, M., Bidichandani, S.I., Hogan, M.E., Patel, P.I., 2001a. Competitive binding of triplex-forming oligonucleotides in the two alternate promoters of the PMP22 gene. Antisense Nucleic Acid Drug Dev 11, 233-246.

Hai, M., Bidichandani, S.I., Patel, P.I., 2001b. Identification of a positive regulatory element in the myelin-specific promoter of the PMP22 gene. J Neurosci Res 65, 508-519.

Hammer, J.A., O'Shannessy, D.J., De Leon, M., Gould, R., Zand, D., Daune, G., Quarles, R.H., 1993. Immunoreactivity of PMP-22, P0, and other 19 to 28 kDa glycoproteins in peripheral nerve myelin of mammals and fish with HNK1 and related antibodies. J Neurosci Res 35, 546-558.

Hanemann, C.O., Gabreels-Festen, A.A., 2002. Secondary axon atrophy and neurological dysfunction in demyelinating neuropathies. Curr Opin Neurol 15, 611-615.

Hanemann, C.O., Gabreels-Festen, A.A., Stoll, G., Müller, H.W., 1997. Schwann cell differentiation in Charcot-Marie-Tooth disease type 1A (CMT1A): normal number of

- myelinating Schwann cells in young CMT1A patients and neural cell adhesion molecule expression in onion bulbs. *Acta Neuropathol* 94, 310-315.
- Haney, C., Snipes, G.J., Shooter, E.M., Suter, U., Garcia, C., Griffin, J.W., Trapp, B.D., 1996. Ultrastructural distribution of PMP22 in Charcot-Marie-Tooth disease type 1A. *J Neuropathol Exp Neurol* 55, 290-299.
- Hasse, B., Bosse, F., Müller, H.W., 2002. Proteins of peripheral myelin are associated with glycosphingolipid/cholesterol-enriched membranes. *J Neurosci Res* 69, 227-232.
- Heinen, A., Kremer, D., Göttle, P., Kruse, F., Hasse, B., Lehmann, H., Hartung, H.P., Küry, P., 2008. The cyclin-dependent kinase inhibitor p57kip2 is a negative regulator of Schwann cell differentiation and in vitro myelination. *Proc Natl Acad Sci U S A*.
- Hromas, R., Broxmeyer, H.E., Kim, C., Nakshatri, H., Christopherson, K., 2nd, Azam, M., Hou, Y.H., 1999. Cloning of BRAK, a novel divergent CXC chemokine preferentially expressed in normal versus malignant cells. *Biochem Biophys Res Commun* 255, 703-706.
- Huehne, K., Rautenstrauss, B., 2001. Transcriptional startpoints and methylation patterns in the PMP22 promoters of peripheral nerve, leukocytes and tumor cell lines. *Int J Mol Med* 7, 669-675.
- Huxley, C., Passage, E., Manson, A., Putzu, G., Figarella-Branger, D., Pellissier, J.F., Fontes, M., 1996. Construction of a mouse model of Charcot-Marie-Tooth disease type 1A by pronuclear injection of human YAC DNA. *Hum Mol Genet* 5, 563-569.
- Huxley, C., Passage, E., Robertson, A.M., Youl, B., Huston, S., Manson, A., Saberan-Djoniedi, D., Figarella-Branger, D., Pellissier, J.F., Thomas, P.K., Fontes, M., 1998. Correlation between varying levels of PMP22 expression and the degree of demyelination and reduction in nerve conduction velocity in transgenic mice. *Hum Mol Genet* 7, 449-458.

- Ip, C.W., Kroner, A., Bendszus, M., Leder, C., Kobsar, I., Fischer, S., Wiendl, H., Nave, K.A., Martini, R., 2006. Immune cells contribute to myelin degeneration and axonopathic changes in mice overexpressing proteolipid protein in oligodendrocytes. *J Neurosci* 26, 8206-8216.
- Irizarry, R.A., Hobbs, B., Collin, F., Beazer-Barclay, Y.D., Antonellis, K.J., Scherf, U., Speed, T.P., 2003. Exploration, normalization, and summaries of high density oligonucleotide array probe level data. *Biostatistics* 4, 249-264.
- Ito, Y., Yamamoto, M., Mitsuma, N., Li, M., Hattori, N., Sobue, G., 2001. Expression of mRNAs for ciliary neurotrophic factor (CNTF), leukemia inhibitory factor (LIF), interleukin-6 (IL-6), and their receptors (CNTFR alpha, LIFR beta, IL-6R alpha, and gp130) in human peripheral neuropathies. *Neurochem Res* 26, 51-58.
- Jessen, K.R., Mirsky, R., 2005. The origin and development of glial cells in peripheral nerves. *Nat Rev Neurosci* 6, 671-682.
- Jetten, A.M., Suter, U., 2000. The peripheral myelin protein 22 and epithelial membrane protein family. *Prog Nucleic Acid Res Mol Biol* 64, 97-129.
- Kadlubowski, M., Hughes, R.A., Gregson, N.A., 1980. Experimental allergic neuritis in the Lewis rat: characterization of the activity of peripheral myelin and its major basic protein, P2. *Brain Res* 184, 439-454.
- Kitamura, K., Suzuki, M., Uyemura, K., 1976. Purification and partial characterization of two glycoproteins in bovine peripheral nerve myelin membrane. *Biochim Biophys Acta* 455, 806-816.
- Kobsar, I., Berghoff, M., Samsam, M., Wessig, C., Maurer, M., Toyka, K.V., Martini, R., 2003. Preserved myelin integrity and reduced axonopathy in connexin32-deficient mice lacking the recombination activating gene-1. *Brain* 126, 804-813.

- Kobsar, I., Hasenpusch-Theil, K., Wessig, C., Müller, H.W., Martini, R., 2005. Evidence for macrophage-mediated myelin disruption in an animal model for Charcot-Marie-Tooth neuropathy type 1A. *J Neurosci Res* 81, 857-864.
- Kobsar, I., Oetke, C., Kroner, A., Wessig, C., Crocker, P., Martini, R., 2006. Attenuated demyelination in the absence of the macrophage-restricted adhesion molecule sialoadhesin (Siglec-1) in mice heterozygously deficient in P0. *Mol Cell Neurosci* 31, 685-691.
- Koenig, H.L., Schumacher, M., Ferzaz, B., Thi, A.N., Ressouches, A., Guennoun, R., Jung-Testas, I., Robel, P., Akwa, Y., Baulieu, E.E., 1995. Progesterone synthesis and myelin formation by Schwann cells. *Science* 268, 1500-1503.
- Kubo, T., Yamashita, T., Yamaguchi, A., Hosokawa, K., Tohyama, M., 2002. Analysis of genes induced in peripheral nerve after axotomy using cDNA microarrays. *J Neurochem* 82, 1129-1136.
- Kuhn, G., Lie, A., Wilms, S., Muller, H.W., 1993. Coexpression of PMP22 gene with MBP and P0 during de novo myelination and nerve repair. *Glia* 8, 256-264.
- Kurth, I., Willimann, K., Schaerli, P., Hunziker, T., Clark-Lewis, I., Moser, B., 2001. Monocyte selectivity and tissue localization suggests a role for breast and kidney-expressed chemokine (BRAK) in macrophage development. *J Exp Med* 194, 855-861.
- Lemke, G., Axel, R., 1985. Isolation and sequence of a cDNA encoding the major structural protein of peripheral myelin. *Cell* 40, 501-508.
- Li, C., Tropak, M.B., Gerlai, R., Clapoff, S., Abramow-Newerly, W., Trapp, B., Peterson, A., Roder, J., 1994. Myelination in the absence of myelin-associated glycoprotein. *Nature* 369, 747-750.

- Li, C., Wong, W.H., 2001. Model-based analysis of oligonucleotide arrays: expression index computation and outlier detection. *Proc Natl Acad Sci U S A* 98, 31-36.
- Liang, G., Cline, G.W., Macica, C.M., 2007. IGF-1 stimulates de novo fatty acid biosynthesis by Schwann cells during myelination. *Glia* 55, 632-641.
- Liehr, T., Rautenstrauss, B., 1995. Regional localization of rat peripheral myelin protein 22 (Pmp22) gene to chromosome 10q22 by FISH. *Mamm Genome* 6, 489.
- Lobsiger, C.S., Magyar, J.P., Taylor, V., Wulf, P., Welcher, A.A., Program, A.E., Suter, U., 1996. Identification and characterization of a cDNA and the structural gene encoding the mouse epithelial membrane protein-1. *Genomics* 36, 379-387.
- Lupski, J.R., de Oca-Luna, R.M., Slaugenhaupt, S., Pentao, L., Guzzetta, V., Trask, B.J., Saucedo-Cardenas, O., Barker, D.F., Killian, J.M., Garcia, C.A., Chakravarti, A., Patel, P.I., 1991. DNA duplication associated with Charcot-Marie-Tooth disease type 1A. *Cell* 66, 219-232.
- Magyar, J.P., Martini, R., Ruelicke, T., Aguzzi, A., Adlkofer, K., Dembic, Z., Zielasek, J., Toyka, K.V., Suter, U., 1996. Impaired differentiation of Schwann cells in transgenic mice with increased PMP22 gene dosage. *J Neurosci* 16, 5351-5360.
- Maier, M., Berger, P., Nave, K.A., Suter, U., 2002a. Identification of the regulatory region of the peripheral myelin protein 22 (PMP22) gene that directs temporal and spatial expression in development and regeneration of peripheral nerves. *Mol Cell Neurosci* 20, 93-109.
- Maier, M., Berger, P., Suter, U., 2002b. Understanding Schwann cell-neurone interactions: the key to Charcot-Marie-Tooth disease? *J Anat* 200, 357-366.
- Manfioletti, G., Ruaro, M.E., Del Sal, G., Philipson, L., Schneider, C., 1990. A growth arrest-specific (gas) gene codes for a membrane protein. *Mol Cell Biol* 10, 2924-2930.

- Martini, R., Schachner, M., Faissner, A., 1990. Enhanced expression of the extracellular matrix molecule J1/tenascin in the regenerating adult mouse sciatic nerve. *J Neurocytol* 19, 601-616.
- Martini, R., Toyka, K.V., 2004. Immune-mediated components of hereditary demyelinating neuropathies: lessons from animal models and patients. *Lancet Neurol* 3, 457-465.
- Mäurer, M., Müller, M., Kobsar, I., Leonhard, C., Martini, R., Kiefer, R., 2003. Origin of pathogenic macrophages and endoneurial fibroblast-like cells in an animal model of inherited neuropathy. *Mol Cell Neurosci* 23, 351-359.
- Meier, C., Parmantier, E., Brennan, A., Mirsky, R., Jessen, K.R., 1999. Developing Schwann cells acquire the ability to survive without axons by establishing an autocrine circuit involving insulin-like growth factor, neurotrophin-3, and platelet-derived growth factor-BB. *J Neurosci* 19, 3847-3859.
- Melcangi, R.C., Magnaghi, V., Cavarretta, I., Zucchi, I., Bovolín, P., D'Urso, D., Martini, L., 1999. Progesterone derivatives are able to influence peripheral myelin protein 22 and P0 gene expression: possible mechanisms of action. *J Neurosci Res* 56, 349-357.
- Melcangi, R.C., Magnaghi, V., Galbiati, M., Ghelarducci, B., Sebastiani, L., Martini, L., 2000. The action of steroid hormones on peripheral myelin proteins: a possible new tool for the rebuilding of myelin? *J Neurocytol* 29, 327-339.
- Meyer Zu Hörste, G., Nave, K.A., 2006. Animal models of inherited neuropathies. *Curr Opin Neurol* 19, 464-473.
- Montag, D., Giese, K.P., Bartsch, U., Martini, R., Lang, Y., Bluthmann, H., Karthigasan, J., Kirschner, D.A., Wintergerst, E.S., Nave, K.A., et al., 1994. Mice deficient for the myelin-associated glycoprotein show subtle abnormalities in myelin. *Neuron* 13, 229-246.

- Morgan, L., Jessen, K.R., Mirsky, R., 1991. The effects of cAMP on differentiation of cultured Schwann cells: progression from an early phenotype (04+) to a myelin phenotype (P0+, GFAP-, N-CAM-, NGF-receptor-) depends on growth inhibition. *J Cell Biol* 112, 457-467.
- Muller, H.W., 2000. Tetraspan myelin protein PMP22 and demyelinating peripheral neuropathies: new facts and hypotheses. *Glia* 29, 182-185.
- Naef, R., Suter, U., 1998. Many facets of the peripheral myelin protein PMP22 in myelination and disease. *Microsc Res Tech* 41, 359-371.
- Nagarajan, R., Le, N., Mahoney, H., Araki, T., Milbrandt, J., 2002. Deciphering peripheral nerve myelination by using Schwann cell expression profiling. *Proc Natl Acad Sci U S A* 99, 8998-9003.
- Niemann, S., Sereda, M.W., Suter, U., Griffiths, I.R., Nave, K.A., 2000. Uncoupling of myelin assembly and schwann cell differentiation by transgenic overexpression of peripheral myelin protein 22. *J Neurosci* 20, 4120-4128.
- Norreel, J.C., Jamon, M., Riviere, G., Passage, E., Fontes, M., Clarac, F., 2001. Behavioural profiling of a murine Charcot-Marie-Tooth disease type 1A model. *Eur J Neurosci* 13, 1625-1634.
- Notterpek, L., Snipes, G.J., Shooter, E.M., 1999. Temporal expression pattern of peripheral myelin protein 22 during in vivo and in vitro myelination. *Glia* 25, 358-369.
- Paratore, C., Hagedorn, L., Floris, J., Hari, L., Kleber, M., Suter, U., Sommer, L., 2002. Cell-intrinsic and cell-extrinsic cues regulating lineage decisions in multipotent neural crest-derived progenitor cells. *Int J Dev Biol* 46, 193-200.

- Pareek, S., Notterpek, L., Snipes, G.J., Naef, R., Sossin, W., Laliberte, J., Iacampo, S., Suter, U., Shooter, E.M., Murphy, R.A., 1997. Neurons promote the translocation of peripheral myelin protein 22 into myelin. *J Neurosci* 17, 7754-7762.
- Pareek, S., Suter, U., Snipes, G.J., Welcher, A.A., Shooter, E.M., Murphy, R.A., 1993. Detection and processing of peripheral myelin protein PMP22 in cultured Schwann cells. *J Biol Chem* 268, 10372-10379.
- Pareyson, D., Schenone, A., Fabrizi, G.M., Santoro, L., Padua, L., Quattrone, A., Vita, G., Gemignani, F., Visioli, F., Solari, A., 2006. A multicenter, randomized, double-blind, placebo-controlled trial of long-term ascorbic acid treatment in Charcot-Marie-Tooth disease type 1A (CMT-TRIAAL): the study protocol [EudraCT no.: 2006-000032-27]. *Pharmacol Res* 54, 436-441.
- Parmantier, E., Cabon, F., Braun, C., D'Urso, D., Muller, H.W., Zalc, B., 1995. Peripheral myelin protein-22 is expressed in rat and mouse brain and spinal cord motoneurons. *Eur J Neurosci* 7, 1080-1088.
- Passage, E., Norreel, J.C., Noack-Fraissignes, P., Sanguedolce, V., Pizant, J., Thirion, X., Robaglia-Schlupp, A., Pellissier, J.F., Fontes, M., 2004. Ascorbic acid treatment corrects the phenotype of a mouse model of Charcot-Marie-Tooth disease. *Nat Med* 10, 396-401.
- Patel, P.I., Roa, B.B., Welcher, A.A., Schoener-Scott, R., Trask, B.J., Pentao, L., Snipes, G.J., Garcia, C.A., Francke, U., Shooter, E.M., Lupski, J.R., Suter, U., 1992. The gene for the peripheral myelin protein PMP-22 is a candidate for Charcot-Marie-Tooth disease type 1A. *Nat Genet* 1, 159-165.

- Perea, J., Robertson, A., Tolmachova, T., Muddle, J., King, R.H., Ponsford, S., Thomas, P.K., Huxley, C., 2001. Induced myelination and demyelination in a conditional mouse model of Charcot-Marie-Tooth disease type 1A. *Hum Mol Genet* 10, 1007-1018.
- Podratz, J.L., Rodriguez, E., Windebank, A.J., 2001. Role of the extracellular matrix in myelination of peripheral nerve. *Glia* 35, 35-40.
- Podratz, J.L., Rodriguez, E.H., Windebank, A.J., 2004. Antioxidants are necessary for myelination of dorsal root ganglion neurons, in vitro. *Glia* 45, 54-58.
- Porter, S., Clark, M.B., Glaser, L., Bunge, R.P., 1986. Schwann cells stimulated to proliferate in the absence of neurons retain full functional capability. *J Neurosci* 6, 3070-3078.
- Privat, A., Jacque, C., Bourre, J.M., Dupouey, P., Baumann, N., 1979. Absence of the major dense line in myelin of the mutant mouse "shiverer". *Neurosci Lett* 12, 107-112.
- Reilly, M.M., 2005. Axonal Charcot-Marie-Tooth disease: the fog is slowly lifting! *Neurology* 65, 186-187.
- Robertson, A.M., Huxley, C., King, R.H., Thomas, P.K., 1999. Development of early postnatal peripheral nerve abnormalities in Trembler-J and PMP22 transgenic mice. *J Anat* 195 (Pt 3), 331-339.
- Robertson, A.M., Perea, J., McGuigan, A., King, R.H., Muddle, J.R., Gabreels-Festen, A.A., Thomas, P.K., Huxley, C., 2002. Comparison of a new pmp22 transgenic mouse line with other mouse models and human patients with CMT1A. *J Anat* 200, 377-390.
- Ryan, M.C., Notterpek, L., Tobler, A.R., Liu, N., Shooter, E.M., 2000. Role of the peripheral myelin protein 22 N-linked glycan in oligomer stability. *J Neurochem* 75, 1465-1474.

- Saberan-Djoneidi, D., Sanguedolce, V., Assouline, Z., Levy, N., Passage, E., Fontes, M., 2000. Molecular dissection of the Schwann cell specific promoter of the PMP22 gene. *Gene* 248, 223-231.
- Sahenk, Z., Nagaraja, H.N., McCracken, B.S., King, W.M., Freimer, M.L., Cedarbaum, J.M., Mendell, J.R., 2005. NT-3 promotes nerve regeneration and sensory improvement in CMT1A mouse models and in patients. *Neurology* 65, 681-689.
- Schachner, M., Martini, R., 1995. Glycans and the modulation of neural-recognition molecule function. *Trends Neurosci* 18, 183-191.
- Scherer, S.S., 1997. The biology and pathobiology of Schwann cells. *Curr Opin Neurol* 10, 386-397.
- Schmid, C.D., Stienekemeier, M., Oehen, S., Bootz, F., Zielasek, J., Gold, R., Toyka, K.V., Schachner, M., Martini, R., 2000. Immune deficiency in mouse models for inherited peripheral neuropathies leads to improved myelin maintenance. *J Neurosci* 20, 729-735.
- Schneider, C., King, R.M., Philipson, L., 1988. Genes specifically expressed at growth arrest of mammalian cells. *Cell* 54, 787-793.
- Schumacher, M., Guennoun, R., Mercier, G., Desarnaud, F., Lacor, P., Benavides, J., Ferzaz, B., Robert, F., Baulieu, E.E., 2001. Progesterone synthesis and myelin formation in peripheral nerves. *Brain Res Brain Res Rev* 37, 343-359.
- Sedzik, J., Kotake, Y., Uyemura, K., 1998. Purification of PASII/PMP22--an extremely hydrophobic glycoprotein of PNS myelin membrane. *Neuroreport* 9, 1595-1600.
- Sendtner, M., Kreutzberg, G.W., Thoenen, H., 1990. Ciliary neurotrophic factor prevents the degeneration of motor neurons after axotomy. *Nature* 345, 440-441.

- Sereda, M., Griffiths, I., Puhlhofer, A., Stewart, H., Rossner, M.J., Zimmerman, F., Magyar, J.P., Schneider, A., Hund, E., Meinck, H.M., Suter, U., Nave, K.A., 1996. A transgenic rat model of Charcot-Marie-Tooth disease. *Neuron* 16, 1049-1060.
- Sereda, M.W., Meyer zu Hörste, G., Suter, U., Uzma, N., Nave, K.A., 2003. Therapeutic administration of progesterone antagonist in a model of Charcot-Marie-Tooth disease (CMT-1A). *Nat Med* 9, 1533-1537.
- Shapiro, L., Doyle, J.P., Hensley, P., Colman, D.R., Hendrickson, W.A., 1996. Crystal structure of the extracellular domain from P0, the major structural protein of peripheral nerve myelin. *Neuron* 17, 435-449.
- Shy, M.E., 2004. Charcot-Marie-Tooth disease: an update. *Curr Opin Neurol* 17, 579-585.
- Shy, M.E., Jani, A., Krajewski, K., Grandis, M., Lewis, R.A., Li, J., Shy, R.R., Balsamo, J., Lilien, J., Garbern, J.Y., Kamholz, J., 2004. Phenotypic clustering in MPZ mutations. *Brain* 127, 371-384.
- Sleeman, M.A., Fraser, J.K., Murison, J.G., Kelly, S.L., Prestidge, R.L., Palmer, D.J., Watson, J.D., Kumble, K.D., 2000. B cell- and monocyte-activating chemokine (BMAC), a novel non-ELR alpha-chemokine. *Int Immunol* 12, 677-689.
- Snipes, G.J., Suter, U., 1995. Molecular anatomy and genetics of myelin proteins in the peripheral nervous system. *J Anat* 186 (Pt 3), 483-494.
- Snipes, G.J., Suter, U., Shooter, E.M., 1993. Human peripheral myelin protein-22 carries the L2/HNK-1 carbohydrate adhesion epitope. *J Neurochem* 61, 1961-1964.
- Snipes, G.J., Suter, U., Welcher, A.A., Shooter, E.M., 1992. Characterization of a novel peripheral nervous system myelin protein (PMP-22/SR13). *J Cell Biol* 117, 225-238.

- Spreyer, P., Kuhn, G., Hanemann, C.O., Gillen, C., Schaal, H., Kuhn, R., Lemke, G., Müller, H.W., 1991. Axon-regulated expression of a Schwann cell transcript that is homologous to a 'growth arrest-specific' gene. *Embo J* 10, 3661-3668.
- Stoffel, W., Boison, D., Bussow, H., 1997. Functional analysis in vivo of the double mutant mouse deficient in both proteolipid protein (PLP) and myelin basic protein (MBP) in the central nervous system. *Cell Tissue Res* 289, 195-206.
- Street, V.A., Bennett, C.L., Goldy, J.D., Shirk, A.J., Kleopa, K.A., Tempel, B.L., Lipe, H.P., Scherer, S.S., Bird, T.D., Chance, P.F., 2003. Mutation of a putative protein degradation gene LITAF/SIMPLE in Charcot-Marie-Tooth disease 1C. *Neurology* 60, 22-26.
- Suter, U., Moskow, J.J., Welcher, A.A., Snipes, G.J., Kosaras, B., Sidman, R.L., Buchberg, A.M., Shooter, E.M., 1992a. A leucine-to-proline mutation in the putative first transmembrane domain of the 22-kDa peripheral myelin protein in the trembler-J mouse. *Proc Natl Acad Sci U S A* 89, 4382-4386.
- Suter, U., Patel, P.I., 1994. Genetic basis of inherited peripheral neuropathies. *Hum Mutat* 3, 95-102.
- Suter, U., Scherer, S.S., 2003. Disease mechanisms in inherited neuropathies. *Nat Rev Neurosci* 4, 714-726.
- Suter, U., Snipes, G.J., 1995. Biology and genetics of hereditary motor and sensory neuropathies. *Annu Rev Neurosci* 18, 45-75.
- Suter, U., Snipes, G.J., Schoener-Scott, R., Welcher, A.A., Pareek, S., Lupski, J.R., Murphy, R.A., Shooter, E.M., Patel, P.I., 1994. Regulation of tissue-specific expression of alternative peripheral myelin protein-22 (PMP22) gene transcripts by two promoters. *J Biol Chem* 269, 25795-25808.

- Suter, U., Welcher, A.A., Ozcelik, T., Snipes, G.J., Kosaras, B., Francke, U., Billings-Gagliardi, S., Sidman, R.L., Shooter, E.M., 1992b. Trembler mouse carries a point mutation in a myelin gene. *Nature* 356, 241-244.
- Takeda, Y., Notsu, T., Kitamura, K., Uyemura, K., 2001. Functional analysis for peripheral myelin protein PASII/PMP22: is it a member of claudin superfamily? *Neurochem Res* 26, 599-607.
- Taylor, V., Welcher, A.A., Program, A.E., Suter, U., 1995. Epithelial membrane protein-1, peripheral myelin protein 22, and lens membrane protein 20 define a novel gene family. *J Biol Chem* 270, 28824-28833.
- ten Asbroek, A.L., Verhamme, C., van Groenigen, M., Wolterman, R., de Kok-Nazaruk, M.M., Baas, F., 2005. Expression profiling of sciatic nerve in a Charcot-Marie-Tooth disease type 1a mouse model. *J Neurosci Res* 79, 825-835.
- Tobler, A.R., Liu, N., Mueller, L., Shooter, E.M., 2002. Differential aggregation of the Trembler and Trembler J mutants of peripheral myelin protein 22. *Proc Natl Acad Sci U S A* 99, 483-488.
- Tobler, A.R., Notterpek, L., Naef, R., Taylor, V., Suter, U., Shooter, E.M., 1999. Transport of Trembler-J mutant peripheral myelin protein 22 is blocked in the intermediate compartment and affects the transport of the wild-type protein by direct interaction. *J Neurosci* 19, 2027-2036.
- Trapp, B.D., Itoyama, Y., MacIntosh, T.D., Quarles, R.H., 1983. P2 protein in oligodendrocytes and myelin of the rabbit central nervous system. *J Neurochem* 40, 47-54.
- Uschkureit, T., Sporkel, O., Stracke, J., Bussow, H., Stoffel, W., 2000. Early onset of axonal degeneration in double (plp^{-/-}mag^{-/-}) and hypomyelinoses in triple (plp^{-/-}mbp^{-/-}mag^{-/-}) mutant mice. *J Neurosci* 20, 5225-5233.

- Uyemura, K., Yoshimura, K., Suzuki, M., Kitamura, K., 1984. Lipid binding activities of the P2 protein in peripheral nerve myelin. *Neurochem Res* 9, 1509-1514.
- Valentijn, L.J., Baas, F., Wolterman, R.A., Hoogendijk, J.E., van den Bosch, N.H., Zorn, I., Gabreels-Festen, A.W., de Visser, M., Bolhuis, P.A., 1992. Identical point mutations of PMP-22 in Trembler-J mouse and Charcot-Marie-Tooth disease type 1A. *Nat Genet* 2, 288-291.
- Vallat, J.M., Sindou, P., Preux, P.M., Tabaraud, F., Milor, A.M., Couratier, P., LeGuern, E., Brice, A., 1996. Ultrastructural PMP22 expression in inherited demyelinating neuropathies. *Ann Neurol* 39, 813-817.
- Verheijen, M.H., Chrast, R., Burrola, P., Lemke, G., 2003. Local regulation of fat metabolism in peripheral nerves. *Genes Dev* 17, 2450-2464.
- Vigo, T., Nobbio, L., Hummelen, P.V., Abbruzzese, M., Mancardi, G., Verpoorten, N., Verhoeven, K., Sereda, M.W., Nave, K.A., Timmerman, V., Schenone, A., 2005. Experimental Charcot-Marie-Tooth type 1A: a cDNA microarrays analysis. *Mol Cell Neurosci* 28, 703-714.
- Wagner-Recio, M., Toews, A.D., Morell, P., 1991. Tellurium blocks cholesterol synthesis by inhibiting squalene metabolism: preferential vulnerability to this metabolic block leads to peripheral nervous system demyelination. *J Neurochem* 57, 1891-1901.
- Welcher, A.A., Suter, U., De Leon, M., Snipes, G.J., Shooter, E.M., 1991. A myelin protein is encoded by the homologue of a growth arrest-specific gene. *Proc Natl Acad Sci U S A* 88, 7195-7199.
- Wu, Z., 2004. A Model-Based Background Adjustment for Oligonucleotide Expression Arrays. *Journal of the American Statistical Association* Volume 99, pp. 909-917(909).

Wulf, P., Bernhardt, R.R., Suter, U., 1999. Characterization of peripheral myelin protein 22 in zebrafish (zPMP22) suggests an early role in the development of the peripheral nervous system. *J Neurosci Res* 57, 467-478.

Zeller, N.K., Hunkeler, M.J., Campagnoni, A.T., Sprague, J., Lazzarini, R.A., 1984.

Characterization of mouse myelin basic protein messenger RNAs with a myelin basic protein cDNA clone. *Proc Natl Acad Sci U S A* 81, 18-22.

7. Abbreviations

BAC	bacterial artificial chromosome
BrdU	5-bromo-2'-deoxy-uridine
cAMP	cyclic adenosine monophosphate
Ccnd1	cyclin D1
CD8, CD34	cluster of differentiation 8, 34
CH	congenital hypomyelination
CMT	Charcot-Marie-Tooth
CMT1, 2, 4	Charcot-Marie-Tooth type 1, 2, 4
CMT1A, 1B, 1C, 1D, 1F	Charcot-Marie-Tooth type 1A, 1B, 1C, 1D, 1F
CMTX	Charcot-Marie-Tooth type X-linked
CNS	central nervous system
CNTF	ciliary neurotrophic factor
CREB	cAMP responsive element binding protein
Ct	cycle threshold
Cx32	connexin 32
CXCL14	CXC ligand 14
DAPI	4',6-diamidino-2-phenylindole
DI-CMT	dominant intermediate Charcot-Marie-Tooth disease
DMEM	Dulbecco's modified Eagle's medium
DNase I	deoxyribonuclease I
DRG	dorsal root ganglia

DSS	Dejerine-Sottas syndrome
EGR2/ KROX20	early growth response 2
EMG	electromyography
Gapdh	glyceraldehyde 3-phosphate dehydrogenase
Gas-3	growth arrest-specific 3
GFP	green fluorescent protein
HMN	hereditary motor neuropathy
HMSN	hereditary motor and sensor neuropathy
HNPP	hereditary neuropathy with liability to pressure palsies
HSAN	hereditary sensory and autonomic neuropathy
LB	Luria-Bertani
LITAF	lipopolysaccharide-induced tumour necrosis factor
MAG	myelin-associated glycoprotein
MBP	myelin basic protein
MCP-1/CC12	monocyte chemotactic protein-1
M-CSF	macrophage colony stimulating factor
MFN2	guanosine triphosphatase mitofusin 2
MPZ	myelin protein zero
NCV	nerve conduction velocity
NEFL	neurofilament light chain
Ninj1	ninjurin 1
PBS	phosphate-buffered saline
PCR	polymerase chain reaction

PMP22	peripheral myelin protein 22
PMP22tg	transgenic <i>PMP22</i> -overexpressing mice of the C61 strain
PNS	peripheral nervous system
qRT-PCR	quantitative RT-PCR
RAG-1	recombination activating gene 1
rCXCL14	recombinant CXCL14
SAGE	serial analysis of gene expression
shRNA	short hairpin RNA
SIMPLE	small integral membrane protein of lysosome/late endosome
TCR α	T-cell receptor α -subunit
Tnc	tenascin C
YAC	yeast artificial chromosome

8. Acknowledgments

I would like to give special thanks to my mentor, Prof. Dr. Hans Werner Müller, for giving me the opportunity to work on a very interesting project. It has been an unique experience that shaped my scientific outlook.

I would like to thank my “Zweitgutachter” Prof. Dr. Heinz Mehlhorn.

I am also grateful to Dr. Patrick Küry, for his continuous technical support and encouragement.

I am indebted to Prof. Dr. Rudolf Martini and Bianca Kohl, from the Department of Neurology of the University of Würzburg, Germany, for the microscopy analyses, and to Bettina Alexandra Buhren for the teased-nerve fibre preparations.

Thanks also to my peers in the Neurochemisches Labor, for their help in the daily laboratory life.

Last but not least, I would like to thank my partner. This study is the result of his support, encouragement, help and love.

Hiermit erkläre ich, die vorliegende Arbeit selbstständig und unter ausschließlicher Verwendung der angegebenen Hilfsmittel und Quellen angefertigt zu haben. Alle Stellen, die aus veröffentlichten und nicht veröffentlichten Schriften entnommen sind, wurden als solche kenntlich gemacht. Diese Arbeit hat in gleicher oder ähnlicher Form noch keiner anderen Prüfungsbehörde vorgelegen.

Düsseldorf, den 16. Oktober 2008

